Energy Strategy Reviews 54 (2024) 101461

Contents lists available at ScienceDirect

Energy Strategy Reviews

journal homepage: www.elsevier.com/locate/esr

A novel efficient energy optimization in smart urban buildings based on optimal demand side management

Bilal Naji Alhasnawi [a,*], Basil H. Jasim [b], Arshad Naji Alhasnawi [c], Firas Faeq K. Hussain [d], Raad Z. Homod [e], Husam Abdulrasool Hasan [f,g], Osamah Ibrahim Khalaf [h], Rabeh Abbassi [i], Bahamin Bazooyar [j,**], Marek Zanker [k], Vladimír Bureš [k], Bishoy E. Sedhom [l]

[a] Department of Electricity Techniques, Al-Samawah Technical Institute, Al-Furat Al-Awsat Technical University, Kufa, 66001, Iraq
[b] Electrical Engineering Department, Basrah University, Basrah, 61001, Iraq
[c] Department of Biology, College of Education for Pure Sciences, Al-Muthanna University, Samawah, 66001, Iraq
[d] College of Engineering, Al-Ayen Iraqi University, Thi-Qar, Iraq
[e] Department of Oil and Gas Engineering, Basra University of Oil and Gas, Basra, 61004, Iraq
[f] Electromechanical Engineering Department, University of Technology, 10066, Baghdad, Iraq
[g] Ministry of Higher Education & Scientific Research, Department of Studies, Planning & Follow-up, Baghdad, 10011, Iraq
[h] Department of Solar, Al-Nahrain Research Center for Renewable Energy, Al-Nahrain University, Jadriya, Baghdad, Iraq
[i] Department of Electrical Engineering, College of Engineering, University of Ha'il, Ha'il City, 81451, Saudi Arabia
[j] Mechanical and Aerospace Engineering, Brunel University London, Uxbridge, UB8 3PH, UK
[k] Faculty of Informatics and Management, University of Hradec Králové, 50003, Hradec Králové, Czech Republic
[l] Electrical Engineering Department, Faculty of Engineering, Mansoura University, Mansoura, 35516, Egypt

ARTICLE INFO

Handling editor: Mark Howells

Keywords:
Moth-flame optimization algorithm (MFOA)
Grasshopper optimization algorithm (GOA)
Microgrid
Electrical appliance
Improved sine cosine algorithm (ISCA)

ABSTRACT

Increasing electrical energy consumption during peak hours leads to increased electrical energy losses and the spread of environmental pollution. For this reason, demand-side management programs have been introduced to reduce consumption during peak hours. This study proposes an efficient energy optimization in Smart Urban Buildings (SUBs) based on Improved Sine Cosine Algorithm (ISCA) that uses the load-shifting technique for demand-side management as a way to improve the energy consumption patterns of a SUBs. The proposed system's goal is to optimize the energy of SUBs appliances in order to effectively regulate load demand, with the end result being a reduction in the peak to average ratio (PAR) and a consequent minimization of electricity costs. This is accomplished while also keeping user comfort as a priority. The proposed system is evaluated by comparing it with the Grasshopper Optimization Algorithm (GOA) and unscheduled cases. Without applying an optimization algorithm, the total electricity cost, carbon emission, PAR and waiting time are equal to 1703.576 ID, 34.16664 (kW), and 413.5864s respectively for RTP. While, after applying GOA, the total electricity cost, carbon emission, PAR and waiting time are improved to 1469.72 ID, 21.17 (kW), and 355.772s respectively for RTP. While, after applying the ISCA Improves the total electricity cost, PAR, and waiting time by 1206.748 ID, 16.5648 (kW), and 268.525384s respectively. Where after applying GOA, the total electricity cost, PAR, and waiting time are improved to 13.72 %, 38.00 %, and 13.97 % respectively. And after applying proposed method, the total electricity cost, PAR, and waiting time are improved to 29.16 %, 51.51 %, and 35.07 % respectively. According to the results, the created ISCA algorithm performed better than the unscheduled case and GOA scheduling situations in terms of the stated objectives and was advantageous to both utilities and consumers. Furthermore, this study has presented a novel two-stage stochastic model based on Moth-Flame Optimization Algorithm (MFOA) for the co-optimization of energy scheduling and capacity planning for systems of energy storage that would be incorporated to grid connected smart urban buildings.

* Corresponding author.
** Corresponding author.
E-mail addresses: bilalnaji11@yahoo.com (B. Naji Alhasnawi), hanbas632@gmail.com (B.H. Jasim), arshad@mu.edu.iq (A. Naji Alhasnawi), raadahmood@yahoo.com (R.Z. Homod), hussam2003hussam@yahoo.com (H.A. Hasan), usama81818@nahrainuniv.edu.iq (O. Ibrahim Khalaf), r.abbassi@uoh.edu.sa (R. Abbassi), b.bazooyar@brunel.ac.uk (B. Bazooyar), marek.zanker@uhk.cz (M. Zanker), vladimir.bures@uhk.cz (V. Bureš), eng_bishoy90@mans.edu.eg (B.E. Sedhom).

https://doi.org/10.1016/j.esr.2024.101461
Received 5 March 2024; Received in revised form 7 June 2024; Accepted 16 June 2024
Available online 4 July 2024

Nomenclature

Abbreviations & Acronyms	
ISCA	Improved Sine Cosine Algorithm
SUBs	Smart Urban Buildings
DSM	Demand-Side Management
UC	User Comfort
GOA	Grasshopper Optimization Algorithm
MFOA	Moth-Flame Optimization Algorithm
MG	Microgrid
DI	Discomfort Index
DG	distributed generation
FCs	Fuel Cells
MTs	Micro-Turbines
PV	Photovoltaic
WTs	Wind Turbines
CMG	Community Microgrid
DERs	distributed generating resources
SG	smart grid
FPS	flat price system
BPSO	Binary Particle Swarm Optimization
SCADA	Supervisory Control and Data Acquisition
MPPT	Maximum Power Point Tracking
DRP	demand response program
IoT	Internet of Things
BSA	Back Tracking search Algorithm
P2P	Peer-to-Peer
MAF	Multi-Agent Framework
PAR	peak-to-average
CoAP	Constricted Application Protocol
DO	Dandelion Optimizer
RTP	Real-time pricing
LDCs	local distribution companies
DERs	distributed energy resources
TOU	Time of Use
ESS	Energy Storage System
Variables & Parameters	
$I_{i,t}^{\text{Gridbuy}}$ and $I_{i,t}^{\text{Gridsell}}$	Buying and selling electricity
$I_{i,l,t}^{\text{Cut}}$	controllable load
$I_{i,t}^{\text{Gridbuy}}$ and $P_{i,t}^{\text{Gridsell}}$	bought and sold electricity
$P_{i,t}^{\text{ESS}}$	energy storage device's power
$E_{\_}$ Cos t	electricity cost
T	periods time
π_t^{Gridbuy} and π_t^{Gridsell}	cost of power bought or sold at moment t
$M_{\_}$ Cos t	PV panel and energy storage device operating costs
$P_{i,t}^{PV}$	PV power produced at moment t
π^{pv} and π^{ESS}	PV panel and energy storage device operating expenses
L	total number of controllable loads
$P_{i,l,t}^{\text{Cut}}$	reduced power
l^{th}	controllable load
ρ_t^{Cut}	weight factor,
λ	emission coefficient of grid-purchased electricity
$P_{i,t}^{Load}$	electricity demand at time t
$P_{i,t}^{ch}$ and $P_{i,t}^{dch}$	energy storage device's charging and discharging powers
$P_{i,t}^{\text{Gridbuy.max}}$ and $P_{i,t}^{\text{Gridsell.max}}$	maximum power value of the electricity a microgrid buys and sells
$E_{i,t}^{ESS}$ and $E_{i,t-1}^{ESS}$	energy of energy storage device at time t or $t-1$
$E_i^{ESS\cdot max}$	maximum energy storage device capacity
$P_i^{ESS\cdot max}$	maximum energy storage device power
$\mathscr{A}_{\mathscr{PV}}$	is a solar panel's area (m^2)
$\mathscr{I}_r(\ell)$	The solar irradiation ($\frac{kW}{m^2}$) at a given time
$\xi_{\mathscr{PV}}$	PV inverter efficiency (%)
$\mathscr{T}emp_f$	The temperature factor
$\mathscr{T}emp_a(\ell)$	outside room temperatures (∘C)
$\mathscr{T}emp_{amb}$	ambient room temperatures (∘C)
$\overline{\mathscr{A}}$	The athematic mean of data
Γ	Role of gamma
η	standard deviation of data
$\mathscr{S}_{\mathscr{PV}}$	PV operating cost
$\mathscr{S}_s$	Levelized cost of PV energy ($\frac{\$}{\boldsymbol{kWh}}$)
$\mathscr{N}_{\mathscr{PVAN}}$	PV energy output (kWh),
$\mathscr{S}_{\mathscr{PV}}$	total PV energy cost
$\mathscr{S}_{sinv}$	PV investment cost ($),

(*continued on next column*)

(*continued*)

$\mathscr{S}_{som}$	PV operation and maintenance cost
$\eta_{\text{،}}$	degradation in PV
$\mathscr{S}_g$	The utility energy cost ($),
$\mathscr{W}_{g\text{،}}(\ell)$	excess micro-grid producing power delivered to utility (***kW***) during time t,
$\mathscr{W}_{g\text{،}}(\ell)$	The utility-paid microgrid power (kW) for time t (hours)
$\varrho(\ell)$	utility pricing signal ($\frac{\$}{\boldsymbol{kWh}}$) at time ***t***.
$\mathscr{N}_g$ ($)	The predicted thermal generators' utility emissions cost
τ	utility generating emission coefficients
App^{α}	appliance that is being switched ON
$App_{W_t}^{d}$	waiting time of a particular appliance d
P_i	stands for the grasshoppers' location
SO_i	social interaction force
GRE_i	gravitational force
W_i	wind advection
d_{ij}	Euclidean distance between the i^{th} and j^{th} grasshoppers
N	number of grasshoppers
s	represents a function that explains the strength of social forces
$\widehat{e_g}$	gravitational constant,
g	unity vector in direction
b_d and lb_d	upper and lower bounds inside the d^{th} dimension
T_d	d^{th} dimension goal (best solution identified)
P_{im}	imported power
P_{ex}	exported power
P_L	load power
P_{RE}	renewable energy generation
FiT	Feeds-in-Tariff
π	Cost of wholesale electricity
$P_{ch,B}$ and $P_{dch,B}$	Battery bank charging and discharging capacity
$P_{ch,SC}$ and $P_{dch,SC}$	Power to charge and discharge from the SC bank
$E_{\frac{B}{SC}}$	The battery or SC bank's energy content
σB/SC	selfdischarge rate of battery/SC bank
$\eta_{ch,\frac{B}{SC}}$ and $\eta_{dch,\frac{B}{SC}}$	battery/SC bank charging and draining efficiency
$P_{ch,\frac{B}{SC}}$ and $P_{dch,\frac{B}{SC}}$	battery/SC bank's charging and discharging capacities
$P_{ch,\frac{B}{SC}}^{max}$ and $P_{dch,\frac{B}{SC}}^{max}$	maximum power of the battery or SC bank for charging and discharging
u_{ch} and u_{dch}	Binary variables are utilized to prevent simultaneous charging and discharge.
N_I	ideal dimensions for the installed inverter
$P_{I,r}$	installed inverter's rated power
$P_{I,\text{ins}}$	capacity of the inverter that is currently installed
N_c	maximum capability of component c
CC, RC, and $O\&M$	Costs of capital, replacement, and upkeep and operation
Q_{life} and Q_{thr}	The storage component's lifetime throughput as well as its annual throughput.
CRF	capital recovery factor
$SPPW$	factor of Single payment present worth
PL	project lifetime
ir	interest rate
CL	component lifetime
SV	salvage value
N_S	maximum capacity of the storage element
C_{exch}^{i}	cost of energy purchased
NPC_B, NPC_{SC}, and NPC_I	current price of the inverter, SC bank, and battery bank
c	a penalty factor that raises the objective function's returned value by a sizable positive constant.
NPV_{exch}	power exchanges value
N_B and N_{SC}	maximum battery and SC bank capacity
$AH_{B/SC}^{min}$	minimum autonomy hour required of battery or SC bank
GOS_{MG}^{min}	minimum grid outage
$P_{B,r}$ and $P_{SC,r}$	rated power of the battery and SC banks
N_B^{max}, N_I^{max}, and N_T^{max}	the maximum capacity of the transformer, inverter, and battery bank at the common coupling point
$P_{RE,ins}$	current installed capacity of the components used in the production of renewable energy
D_{ij}	distance among moth i and flame j
$S(M_i, F_j)$	spiral function of moth i and flame j
r	a random integer between −1 and 1.
b	a parameter that establishes the logarithmic spiral's form

1. Introduction

To acquire secure, dependable, and clean energy, the outdated grid infrastructure needed to be improved and modernized due to the surge in worldwide electrical energy production and consumption as well as the quick integration of intermittent renewable sources. As a result, the idea of the "smart grid" has come into being, whereby all participants in the grid network communicate and collaborate with one another via information and communication technologies (ICTs) in order to enhance sustainability, resource efficiency, and stability in the fields of energy production, transmission, and distribution. In order to regulate residential end-users' electrical energy consumption—who account for 26.9 % of global electricity final consumption—residential demand-side management, or DSM, is linked to the smart grid idea [1].

All short-term actions intended to alter end users' consumption patterns in the form of peak cutting, valley filling, or load shifting in order to satisfy a load shape required by the electrical grid are collectively referred to as demand response (DR), a tool for demand-side management. Load-serving entities (LSEs) use advanced metering infrastructure (AMI) to provide end-users with financial incentives or time-dependent pricing to facilitate direct load control (DLC) or indirect load control (ILC) as part of residential DR. In DLC, end customers give LSEs permission to remotely operate their appliances, primarily for frequency management or peak shaving, in exchange for rewards [2,3].

Systems for responding to demand offer a flexible and efficient way to balance the supply and demand of power. Demand response systems can be added to microgrids to maximize the use of renewable energy sources. By allowing the supply and demand for power to be balanced, it eliminates the need for expensive energy reserves. Microgrids, as opposed to traditional reserve units, offer a more steady and balanced electrical supply by actively monitoring and reacting to variations in demand. SUBs has garnered significant attention due to its critical role in the construction of future smart grids, and in recent years, there has been a rising number of relevant research projects. Demand-side management was first proposed by the authors in Ref. [4] as a requirement for the profitable operation of home and rural microgrid systems. The application of firefly hybridization with particle swarm optimization in DSM research was described by the authors in Ref. [5].

The authors of [6] provided a real-time community microgrid scheduling system. In the event of a power loss, the authors of [7] offered a unique method for scheduling distributed generating resource (DER) to serve loads inside a micro grid (MG). In order to solve the demand-side management (DSM) issue, the authors of [8] proposed a method for logically distributing energy consumption in the smart grid (SG) by utilizing a flat price system (FPS). The authors presented a novel solution for optimized energy management systems in Ref. [9], which included an AC/DC hybrid microgrid system for industries. The authors presented a novel approach to achieve mppt for photovoltaic system based SCADA in Ref. [10]. The authors presented their efficient optimization algorithm-based demand-side management program for smart grid residential load in Ref. [11]. In Refs. [12–15], writers offered a control method for inverters that run in parallel for use in environmentally friendly applications. Since solar and tidal energy are commonly utilized in power networks as renewable resources, renewable-based microgrids (MGs) have access to a demand response program (DRP), which was made accessible in Ref. [16]. The authors of [17] put up a plan for controlling household energy use those accounts for uncertainty and uses workable demand response techniques. The authors developed a unique internet of energy optimal multi-agent control system in Refs. [18–20] for microgrids that include renewable energy resources. The authors of [21] described energy management in microgrids using deep reinforcement learning and specialized knowledge. A novel Internet of Things-based optimization method for a home demand side management system based on BPSO and BSA was created by the authors in Refs. [22,23]. A novel decentralized control approach for microgrids in the internet of energy framework was given by the authors in Ref. [24].

The authors in Ref. [25] offered power demand control scenarios for smart grid applications with a restricted number of appliances. An algorithm focused on planning the smart device problem for sparing load change in demand management was proposed by the authors in Ref. [26]. The ease of a load transfer reduces consumer annoyance. Using an Internet of Things (IoT)-based bald eagle search optimization technique, the authors of [27] proposed a unique solution for day-ahead scheduling challenges. To encourage a smart grid usage culture, the authors of [28] proposed developing a cloud-based Multi-Agent Framework (MAF) for residential microgrids (RMG). Reducing peak load and energy expenditures associated with intelligent homes is the aim of the micro grid and intelligent home agents described in the MAS. The authors of [29] introduced multi-objective scheduling based on arithmetic optimization approaches for energy management in Internet of Things (IoT) enabled smart homes. In Ref. [30], the author developed a P2P architecture for building islanded microgrids. Multi-layered, multi-agent systems and procedures that accomplish several goals enable P2P development. Agents proficient in data processing and transmission can perform these concurrent tasks linked to multi-layer control. Using effective DSM approaches, the authors of [31] investigated the peak-to-average (PAR) ratio of the grid energy consumption. They examine several aspects such as weather, power pricing, energy use trends, and others to determine the best load management method for flattening the load curve. It provides an energy management strategy based on genetics. An example of a Raspberry Pi3-powered SCADA--controlled smart home was given by the authors of [32]. The authors described a fog-based internet of energy architecture in Ref. [33] for transactive energy management systems.

The authors introduced a new on-grid/off-grid energy management system in Ref. [34] that uses an adaptive neuro-fuzzy inference method. An energy management system for demand-side control in smart grids based on cloud computing and the Internet of Things was presented by the authors of [35]. Utility companies and consumers can both remotely access a consumer recharge profile by using this device. Consumer load profiles can help businesses control, offer incentives to, and convince customers to reduce their energy usage. A multi-agent system based on demand response was developed and implemented in Ref. [36] for active network control of delivery networks. The project's objective is to supply dynamic boards to distribution network operators and distribution system operators (DSOs) as a practical and efficient means of communication. The authors of [37] presented hierarchical EMS, which was optimization-based. A novel agent-based paradigm that integrates the adaptable features of home and work environments has been developed by the authors of [38]. A task scheduling system for multi-objective demand response to real-time prices (RTP) was presented by the authors of [39].

Instead of examining the optimal BOA-based DSMS operation, the authors of [40] created a SEMS as a service for nanogrid equipment used in cloud computing platforms. An adaptive power management method for both grid mode and insulated mode was published by the authors of [41]. In this study, demand is satisfied in the client's home area through the employment of a hybrid system that combines photovoltaics, batteries, and energy distribution. When necessary, the coordinated energy delivery services can supply active power and the appropriate quantity of service thanks to the suggested approach. The authors of [42] provided a framework for energy management (EMS) in smart homes. This gadget establishes a wireless network of many devices on each home computer by connecting to an IP address-based Internet of Things (IoT) module. The author's operational state models and flexible load are provided in Ref. [43]. In southern Anhui, load scheduling was employed to maximize the variable load of residential buildings while taking current power costs and renewable energy generation into consideration. The optimization process's goal was to lower the buying price. A novel binary backtracking search algorithm-based real-time optimal scheduling controller for a home energy management system was

presented by the authors of [44]. For an islanded power system with scattered energy supplies, the authors of [45] proposed the ideal load-shedding technique based on the grasshopper optimization algorithm.

The authors published their presentation, "Energy management in smart cities based on the internet of things: peak demand reduction and energy savings," in Ref. [46]. A novel real-time electricity scheduling for home energy management system using the internet of energy was presented by the authors in Ref. [47]. The developers of [48] offer a distinct fog computing network service for power management. The adoption of the fog computing platform facilitates real-time energy management, data protection, accessibility, flexibility, and interoperability. The authors presented a self-learning home management architecture in Ref. [49]. The Internet of Things concepts were combined for agent interaction and communication using a Multi-Agent System platform. An inventive, dependable EMS and control method for a hybrid microgrid system powered by green energy was proposed by the authors of [50]. A real-time monitoring interface was employed by the authors of [51] to define an enhanced microgrid energy management strategy. The authors initially introduced consensus negotiation-based decision making in Ref. [52] for connected appliances in smart home management systems. In Ref. [53], the authors described an effective demand response program and renewable energy sources for smart grid energy management. The authors provided a multi-objective enhanced cockroach swarm algorithm technique in Ref. [54] for residential energy management systems. The authors of [55] proposed utilizing the ITS-BF algorithm to schedule residential units' electrical appliances for the following day in a smart home network. For internet-of-energy-based smart homes, the authors of [56] provided a thorough strategy for intelligent energy management and demand reduction.

The authors in Ref. [57] covered the integration of control methods for integrating a grid-connected wind-photovoltaic hybrid system with adaptation converters coupled to a shared DC bus. In order to minimize costs, the authors of [58] described how to size renewable energy systems with microgrids based on energy storage systems using hybrid shuffling, frog-leaping, and pattern search algorithms. The authors of [59] proposed energy management and optimal operation of renewable energy sources and electric vehicles based on microgrid by using a hybrid gravitational search and pattern search method. The authors suggested the hybrid crow and pattern search algorithm in Ref. [60] as a cost-oriented resource scheduling technique for a solar-powered microgrid. The authors of the study in Ref. [61] suggest a novel Dandelion Optimizer (DO) to precisely determine the PEMFC model's parameters for the first time. Improved off-grid wind, PV, and hybrid energy storage system based on novel Moth-Flame optimization algorithm framework was proposed by the authors in Ref. [62]. By zoning the network into many clusters, the authors of [63] presented a zonal-based optimal microgrid identification model with the goal of determining the ideal microgrid topology in the current distribution systems. The integrated utility grid system was the main focus of the authors of [64]. A novel technique for managing a DPGS's grid side inverter is developed, accounting for an unbalanced grid. For a microgrid that includes renewable energy sources, the authors in Refs. [65–71] developed a day-ahead combined energy management and battery size framework based on the β-modified krill herd algorithm.

The vehicle-to-home idea was integrated into one of the two residential microgrids compared by the authors of [72], providing a case study that highlights the attractiveness of this technology for households. The authors of [73] introduced the coalitions-game theory for energy management schemes in intelligent microgrids, which is based on the consensus algorithm. By employing renewable energy resources, the authors of [74] developed a novel technique for coordinating the operation of hybrid microgrids with changing loads and generating circumstances. In Ref. [75] the authors presented the modeling and design of a modular energy management system and its integration into a grid-connected battery-based microgrid. In the stand-alone system, the authors of [76] provide a novel economic dispatch using an improved butterfly optimization technique. Authors of [77] presented a method for demand side management in smart homes that integrates energy optimization with microgrid operations. Multiple HEMS simultaneously optimize their individual energy consumption patterns and calculate their flexibility provision, which is conveyed to the local distribution companies (LDCs), according to a two-stage optimization paradigm proposed in Ref. [78]. Distributed energy management of the hybrid AC/DC microgrid with high penetration of distributed energy resources based on ADMM was given by the authors in Ref. [79]. The authors of [80] introduced a multi-objective optimization technique for solar and battery energy storage in household energy management systems. Authors of [81] presented a time-of-use tariff plan for Bangladeshi residential energy consumers to regulate their consumption.

The demand side management strategy for smart buildings utilizing the multi-objective hybrid optimization technique was given by the authors in Ref. [82]. In Ref. [83] the authors presented a Flexible demand-side management program in accordance with the consumers' requested constraints.

In [84] the authors presented Optimization-based optimal energy management system for smart home in smart grid. Deep learning-assisted distributed fiber optic sensors for intelligent monitoring of spatially distributed cracks was presented by the authors in Ref. [85]. The authors published a review on machine learning-based automated condition assessment of pipelines in Ref. [86]. The authors of [87] presented the use of heterogeneous signal characteristics acquired from utterance-based parallel neural networks for audio sentiment analysis. The authors of [88] described the complimentary merging of many modalities and multiple characteristics in sentiment analysis. The authors presented a deep learning-based method for classifying macromolecules using unbalanced data from cellular electron cryotomography in Ref. [89].

1.1. Research gap of related works

While extensive research has been conducted on reducing peak-to-average ratio (PAR), energy costs, and improving customer savings and utility benefits in Time-of-Use (ToU) pricing, several gaps remain.

- In many systems like [81], and [100], the authors did not use a metaheuristic technique (e.g., Improved Sine Cosine Algorithm (ISCA) and the Grasshopper Optimization Algorithm (GOA), etc.) to minimizes Electricity Cost (EC) and Peak to Average Ratio (PAR) while maximizing User Comfort (UC).
- In many papers, accuracy is enhanced at expense of increased complexity of system.
- In many papers, a stable, accurate, and efficient performance is achieved at the cost of high execution time.
- Some literatures did not consider the trade-offs between minimizing electricity bills and user discomfort.
- Absence of a two-stage stochastic model based on the Moth-Flame Optimization Algorithm (MFOA) for co-optimizing energy storage system capacity planning and scheduling in grid-connected medium-sized generators (MGs).

1.2. Contributions of this work

- This paper presents an efficient energy optimization in smart urban buildings based on Improved Sine Cosine Algorithm (ISCA) and the Grasshopper Optimization Algorithm (GOA)
- The article seeks to accomplish a number of contradictory goals, such as reducing energy costs, increasing the total amount of requests for approved power, reducing CO2 emissions, and maximizing the total amount of requests for authorized power.
- To overcome a number of obstacles and improve the overall effectiveness of the study, ISCA is suggested. A number of simulations are

carried out to validate the results. The effectiveness of the recommended methodology is validated by looking at performance indicators that offer significant cost savings with a low chance of unfavorable events for the user.

- The results obtained via proposed methodology are compared to a number of existing techniques. Also, savings in electricity bills for various consumer categories are estimated.
- Analyzes the impact of battery storage on appliance operation times and grid balancing.
- Develops a novel two-stage stochastic model for co-optimizing energy storage system capacity planning and scheduling in grid-connected MGs using the MFOA.

2. Proposed system

Installing a small-scale photovoltaic energy storage system has become vital for every family in Smart Urban Buildings due to the exponential expansion of distributed energy. The system structure diagram for a smart urban building based on an energy management system is displayed in Fig. 1. Evidently, each managed load is linked to a smart socket, which the SUBs may control directly. The controlled load can be turned on or off when the smart socket receives a signal from the SUBs. One way to respond to demand for electricity is to reduce or modify one's usage. The primary study items in this investigation are energy storage devices and changeable loads. Reducing partially controllable loads and scheduling energy storage devices are the main goals of this article in order to lower carbon emissions and Smart Urban Buildings power costs. The model accounts for the exchange of electricity between Smart Urban Buildings and the grid in the interim. This section describes the specific choice variables, the model's objective functions and constraints, and the energy storage device's approach to handling limitations.

2.1. Factors that influence decisions

The Smart Urban Buildings (SUBs) model's six different characteristic categories are selected as the choice factors in order to get the best solution for electricity usage:

$$C = \left[I_{i,t}^{\text{Gridbuy}}, I_{i,t}^{\text{Gridsell}}, I_{i,l,t}^{\text{Cut}}, P_{i,t}^{\text{Gridbuy}}, P_{i,t}^{\text{Gridsell}}, P_{i,t}^{\text{ESS}} \right] \quad (1)$$

The time period index (t), SUB residence index (i), and controllable load index l are represented in this example. Electrical energy purchasing and selling are represented by the binary variables $I_{i,t}^{\text{Gridsell}}$ and $I_{i,t}^{\text{Gridbuy}}$ respectively. The binary variable $I_{i,l,t}^{\text{Cut}}$ represents the controllable load's operational condition. The variables $I_{i,t}^{\text{Gridbuy}}$ and $P_{i,t}^{\text{Gridsell}}$ in the microgrid stand for the power that was bought and sold at time t, respectively. $P_{i,t}^{\text{ESS}}$ denotes the power being charged or discharged by the microgrid's energy storage device at time t [90].

2.2. Objective functions

To maximize the economic and social benefits of Smart Urban Buildings consumption, optimization objectives are given for energy cost, DR curtailment value, and carbon emissions while accounting for

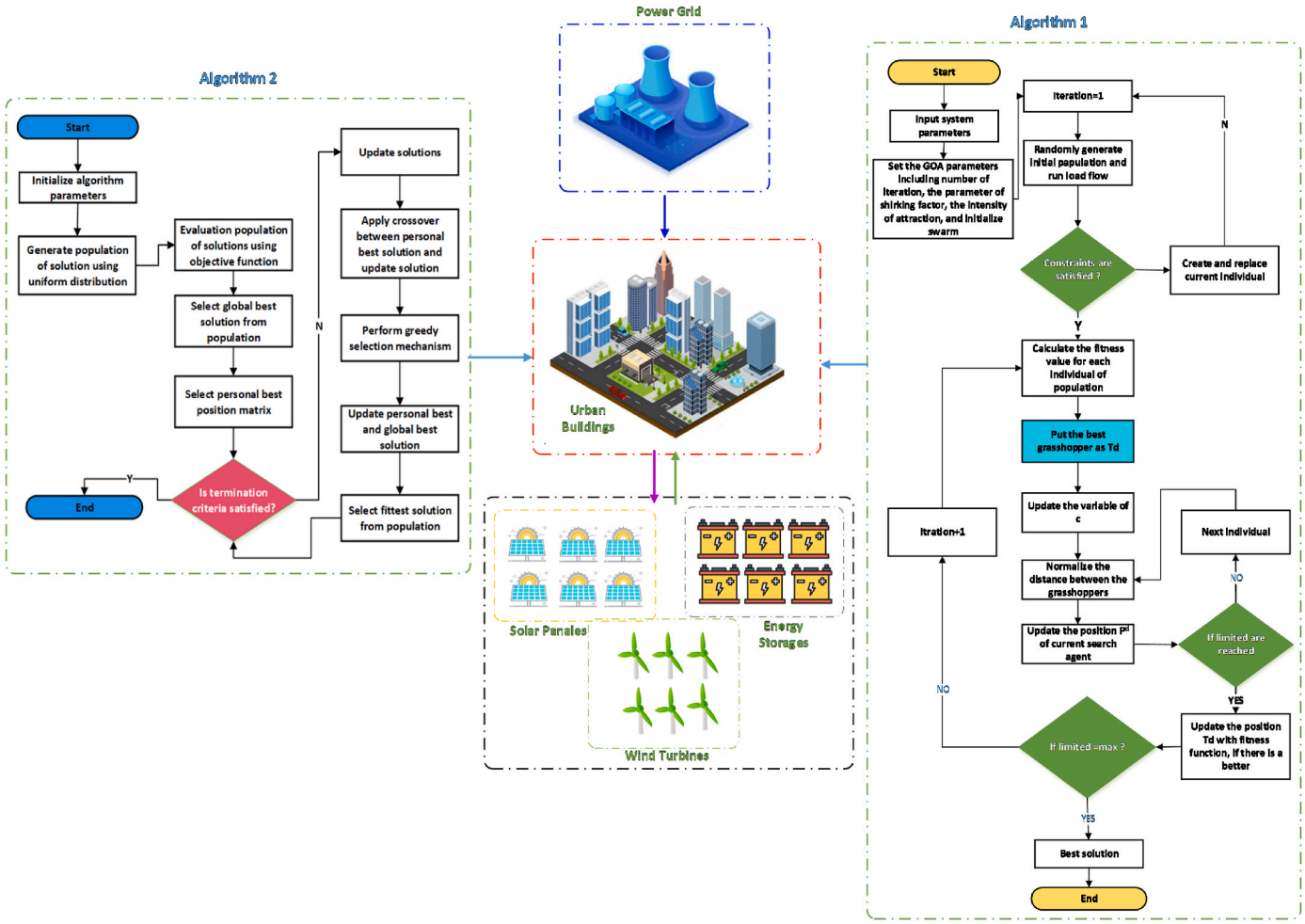

Fig. 1. Suggested smart urban buildings system.

inhabitants' electrical economy, DR participation, and environmental indicators.

2.2.1. Cost of electricity

The definition of the electricity cost goal function includes the price of purchasing power for the family, the revenue from selling electricity, and the running costs of photovoltaic panels and energy storage devices:

$$E\_Cost = \sum_{i=1}^{I}\sum_{t=1}^{T}\left(I_{i,t}^{Gridbuy} \times P_{i,t}^{Gridbuy} \times \pi_t^{Gridbuy} - I_{i,t}^{Gridsell} \times P_{i,t}^{Gridsell} \times \pi_t^{Gridsell}\right) \times \frac{1}{\Delta t} + M\_Cost \quad (2)$$

where T is total number of hours in a day, and the electricity cost is represented by $E\_$ Cos t. Let I be the total number of SUB; let Δt be the total number of 1-h time intervals, each lasting 15 min. At every given moment t, the prices of power bought and sold are represented, respectively, by π_t^{Gridsell} and π_t^{Gridbuy}. PV panel and device of energy storage operating expenses are stated in terms of $M_$Cost, which is calculated as follows:

$$M\_Cost = \sum_{i=1}^{I}\sum_{t=1}^{T}\left(P_{i,t}^{PV} \times \pi^{pv} + \left|P_{i,t}^{ESS}\right| \times \pi^{ESS}\right) \times \frac{1}{\Delta t} \quad (3)$$

where $P_{i,t}^{PV}$ stands for photovoltaic power generated at t. Operating costs of solar panel and energy storage device are denoted by the symbols π^{pv} and π^{ESS}.

2.2.2. DR restriction's value

By reducing partial loads, the DR curtailment value—which has the following definition—is utilized to measure resident involvement in the DR program:

$$DR_{Value} = \sum_{i=1}^{I}\sum_{t=1}^{T}\sum_{l=1}^{L}\left(P_{i,l,t}^{Cut} \times I_{i,l,t}^{Cut} \times \rho_t^{Cut}\right) \times \frac{1}{\Delta t} \quad (4)$$

In this case, *DR_Value* is the DR curtailment value, $P_{i,l,t}^{\text{Cut}}$ is the DR curtailment value, and L is total number of controlled loads. The load's power at time t is equal to the l^{th} controlled load's reduced power. Weight factor, ρ_t^{Cut} is configured to reduce partial loads.

2.2.3. Emissions of carbon

Achieving low-carbon electricity use for residents is important because CO_2 emissions have a significant green Smart Urban Buildings effect on the environment. The following is the definition of the carbon emission objective function:

$$Envir_{CO_2} = \lambda \times \sum_{i=1}^{I}\sum_{t=1}^{T}\left(I_{i,t}^{Gridbuy} \times P_{i,t}^{Gridbuy}\right) \times \frac{1}{\Delta t} \quad (5)$$

where λ, the emission coefficient of power purchased from the grid, has a value of 0.785 kg CO_2/kWh, and *Envir_*CO_2 represents carbon emission.

2.3. Restrictions

The following constraints apply to the schedule optimization model in order to provide regular exchanges between Smart Urban Buildings and the grid.

2.3.1. Limitations on equilibrium power

The power balance equation can be represented as follows;

$$P_{i,t}^{G\ ridbuy} + P_{i,t}^{PV} + P_{i,t}^{dch} = P_{i,t}^{Load} + P_{i,t}^{ch} + P_{i,t}^{G\ ridsell} \quad (6)$$

The energy storage device's charging and discharging powers are represented by $P_{i,t}^{ch}$ and $P_{i,t}^{dch}$, respectively, and are defined as follows: $P_{i,t}^{Load}$ represents the electricity demand at time t:

$$P_{i,t}^{ch} = P_{i,t}^{ESS}, \&\& P_{i,t}^{ESS} > 0 \quad (7)$$

$$P_{i,t}^{dch} = P_{i,t}^{ESS}, \&\& P_{i,t}^{ESS} < 0 \quad (8)$$

2.3.2. Limitations on inequality

- *Limitations on Operating State with Controlled Load*:

$$0 \le I_{i,l,t}^{Cut} \le 1 \quad (9)$$

- Electricity purchase and sale constraint:

$$0 \le I_{i,t}^{Gridbuy} + I_{i,t}^{Gridsell} \le 1 \quad (10)$$

- Restrictions on the power of electricity that is bought and sold:

$$0 \le P_{i,t}^{Gridbuy} \le P_{i,t}^{Gridbuy.max} \quad (11)$$

$$0 \le P_{i,t}^{Gridsell} \le P_{i,t}^{Gridsell.max} \quad (12)$$

In this case, $P_{i,t}^{\text{Gridbuy.max}}$ and $P_{i,t}^{\text{Gridsell.max}}$ stand for the highest power value that microgrids can buy and sell, respectively.

2.4. Energy-storing

Because the energy storage device buffers the electricity used in Smart Urban Buildings, it is important to account for the financial and environmental aspects of charging and discharging the device. Storage device's mathematical model is as follows:

$$E_{i,t}^{ESS} = E_{i,t-1}^{ESS} + P_{i,t}^{ESS} \times \frac{1}{\Delta t} \quad (13)$$

$$0 \le E_{i,t}^{ESS} \le E_i^{ESS\cdot max} \quad (14)$$

$$-P_i^{ESS\cdot max} \le P_{i,t}^{ESS} \le P_i^{ESS\cdot max} \quad (15)$$

where $E_{i,t}^{ESS}$ and $E_{i,t-1}^{ESS}$, respectively, indicate the energy of storage device at times t and $t-1$; $E_i^{ESS\cdot max}$ and $P_i^{ESS\cdot max}$ represent the energy storage device's maximum capacity and power, respectively. The capacity constraint on the energy storage device makes fixing the constraints challenging during the algorithm's optimization stage. The direct repair method was employed in this work to solve the limitation and produce more workable solutions. Here is how the repair process is defined:

$$E_{i,t}^{ESS} = \begin{cases} 0, E_{i,t}^{ESS} < 0 \\ E_i^{ESSmax}, E_{i,t}^{ESS} > E_i^{ESS\cdot max} \\ E_{i,t}^{ESS}, otherwise \end{cases} \quad (16)$$

$$P_{i,t}^{ESS} = \begin{cases} E_{i,t}^{ESS} - E_{i,t-1}^{ESS}, E_{i,t}^{ESS} < 0 \\ E_{i,t}^{ESS} - E_{i,t-1}^{ESS}, E_{i,t}^{ESS} > E_i^{ESSmax} \\ P_{i,t}^{ESS}, otherwise \end{cases} \quad (17)$$

where Equation (17) describes what should happen if the energy storage capacity limit is exceeded, and Equation (18) illustrates what should happen if power is charged or discharged.

2.5. Photovoltaic system

The output power, $\mathscr{W}_{\mathscr{P}\mathscr{V}}$ (kW), of the installed rooftop PV system is expressed in micro grid as follows [91].

$$\mathscr{W}_{\mathscr{P}\mathscr{V}}(\ell)=\xi_{\mathscr{P}\mathscr{V}}\times\mathscr{A}_{\mathscr{P}\mathscr{V}}\times\mathscr{I}_{r}(\ell)\left[1-\mathscr{T}emp_{f}(\mathscr{T}emp_{a}(\ell)-\mathscr{T}emp_{amb})\right] \tag{18}$$

$$\mathscr{W}_{min}\le\mathscr{W}_{\mathscr{P}\mathscr{V}}\le\mathscr{W}_{max} \tag{19}$$

where $\mathscr{A}_{\mathscr{P}\mathscr{V}}$ is a solar panel's area ($\boldsymbol{m^2}$), $\mathscr{I}_{r}(\ell)$ is the solar irradiation ($\frac{\boldsymbol{kW}}{\boldsymbol{m^2}}$) at a given time, and $\boldsymbol{\xi}_{\mathscr{P}\mathscr{V}}$ is the PV inverter efficiency (%). The temperature factor is $\mathscr{T}emp_{f}$, while the outside and ambient room temperatures (∘C) are represented by $\mathscr{T}emp_{a}(\ell)$ and $\mathscr{T}emp_{amb}$.

The PV output power hourly distribution (WPDF) likelihood is computed and assessed using the Weibull probability density function. Next, the shape and scale parameters of the WPDF are used to validate the PV model. The PV output power's WPDF is as follows:

$$\mathscr{f}(\mathscr{W}_{\mathscr{P}\mathscr{V}}(\ell))=\frac{k}{c}\times\left(\frac{\mathscr{I}_{r_r}(\ell)}{c}\right)^{k-1}\times e^{-\left(\frac{I_r(t)}{c}\right)^{k}} \tag{20}$$

$$k=\left(\frac{\eta}{\overline{\mathscr{A}}}\right)^{-1.086},\ and\ \ c=\frac{\overline{\mathscr{A}}}{\Gamma\left(1+\frac{1}{k}\right)} \tag{21}$$

where $\overline{\mathscr{A}}$ is the data's mathematical mean, $\boldsymbol{\eta}$ is the data's standard deviation, and Γ is the gamma function.

The following methods can be used to simulate the PV running cost ($\mathscr{S}_{\mathscr{P}\mathscr{V}}$) and levelized PV energy cost ($\mathscr{S}_{s}$) ($\frac{\$}{\boldsymbol{kWh}}$) over the course of the system lifespan, respectively.

$$\mathscr{S}_{s}=\frac{\mathscr{S}_{sinv}+\sum_{i=1}^{n}\mathscr{S}_{som}(1+\mathscr{E}_{r})^{-\ell}}{\sum_{i=1}^{n}\mathscr{N}_{\mathscr{P}\mathscr{V}\mathscr{A}\mathscr{N}}(1-\eta_{s})^{\ell-1}} \tag{22}$$

$$\mathscr{S}_{\mathscr{P}\mathscr{V}}=\sum_{\ell=1}^{\mathscr{T}}\mathscr{S}_{s}\times\mathscr{W}_{\mathscr{P}\mathscr{V}}(\ell)\mathscr{f}(\mathscr{W}_{\mathscr{P}\mathscr{V}}(\ell)) \tag{23}$$

where n is the PV lifetime, $\mathscr{S}_{som}$ is the PV operation and maintenance cost $\mathscr{S}_{sinv}$ is the PV investment cost ($), and $\mathscr{S}_{\mathscr{P}\mathscr{V}}$ is the total PV energy cost. The annual PV energy output (kWh) is denoted by $\mathscr{N}_{\mathscr{P}\mathscr{V}\mathscr{A}\mathscr{N}}$. The PV degradation is represented by $\boldsymbol{\eta}_{s}$.

2.6. Utility grid

RES and ESS are examples of private supply sources that are linked to the utility during times when the microgrid's demand is at its highest. Conversely, the electricity generated by the microgrid is provided to the utility at the utility rate during off-peak hours. A contract between the utility and the owner of the microgrid is necessary in order for the utility to be able to buy the excess energy from the microgrid. As a result, the generating units' energy costs and $\boldsymbol{CO_2}$ emissions expenses will go down. To increase dependability and meet demand, the deal also permits the utility to sell SMG its electricity. The utility energy cost $\mathscr{S}_{g}$ ($), based on the price signal, is provided as [92]:

$$\mathscr{S}_{g}=\sum_{\ell=1}^{\mathscr{T}}\left[\mathscr{W}_{gc}(\ell)-\mathscr{W}_{gs}(\ell)\right]\varrho(\ell) \tag{24}$$

where $\mathscr{W}_{gs}(\ell)$ is excess micro-grid producing power delivered to utility ($\boldsymbol{kW}$) during time $\boldsymbol{t}$. The utility pricing signal ($\frac{\$}{\boldsymbol{kWh}}$) at time $\boldsymbol{t}$ is represented by $\boldsymbol{\varrho(t)}$, and $\mathscr{W}_{gc}(\ell)$ is microgrid power paid from utility (kW) during that period. The predicted thermal generators' Cost of utility emissions, $\mathscr{N}_{g}$ ($), is calculated as follows:

$$\mathscr{N}_{g}=\sum_{\ell=1}^{\mathscr{T}}\left[\sigma\left(\mathscr{W}_{gc}(\ell)\right)^{2}+\varsigma\mathscr{W}_{gc}(t)+\tau\right] \tag{25}$$

where $\boldsymbol{\tau}$ represents utility generating emission coefficients.

2.7. Smart appliances

SUB dwellings have three different kinds of loads: hybrid, non-interruptible, and interruptible. Batteries, water heaters, air conditioners, and dishwashers can all be grouped according to the user's lifestyle. Appliances of the first class have a programmable work cycle. On the other hand, appliances that are non-interruptible cannot have their use postponed. Operational limitations and mathematical modeling of the main domestic appliances are covered here. The amount of time that each appliance must run is decided by Ref. [93]:

$$O_{i}(t)=\begin{cases}1 & if\ t\in\tau_{i},\forall,i\in A,\\ 0 & otherwise\end{cases} \tag{26}$$

Water heaters and air conditioners are examples of appliances that operate to maintain temperatures within set ranges. Therefore, the following conditions have to be satisfied in order to accurately portray this equipment.

$$T_{min}\le T_{req}\le T_{max},\forall t\in\tau_{i},i\in\{AC,wh\} \tag{27}$$

$$O_{i}(1)=\begin{cases}1,if\ T_{i}(0)>T_{i}(1), & i\in\{ac,wh\}\\ 0,if\ T_{i}(0)<T_{i}(1), & i\in\{ac,wh\}\end{cases} \tag{28}$$

In this instance, Equation (27) guarantees that thermal appliances function within temperature ranges that the user has selected, and Equation (28) guarantees that an appliance will first switch on if its temperature surpasses the upper limit before the model initialization; if not, it will stay in the off state. Apart from the aforementioned limitations, every appliance is associated with a specific mathematical equation that illustrates its functioning; this is addressed in the subsequent sections.

2.7.1. Air condition

The model considers all the significant factors that can affect cooling, including activity level, the temperature difference between the indoor and outdoor settings, and the number of occupants, in order to maintain the air conditioning temperature within a given range. The air conditioning system's operational limitations are shown in the following equation:

$$T_{final}(t)=T_{ini}(t-1)+\mu(T_{out}(t)-T_{int}(t))+\mu(\beta(t)+\zeta)+\mu O_{i}(t)\forall t=\tau,i=ac \tag{29}$$

Equation (29), which illustrates how the AC interior temperature changes over time. The formula shows how the indoor temperature is affected at specific intervals by the initial temperature, the amount of activity in the Smart Urban Buildings, the difference in temperature between the inside and outside, and whether an appliance is on. The cooling effect of the air conditioner in its ON state is represented via beta. μ represents the effect of population density, activity level, and temperature differential on a given temperature, respectively. The temperature threshold, or the upper and lower bounds at which customers can tolerate temperature variation, is another factor considered by the model.

2.7.2. Water heater

The quantity of hot water utilized in different microgrids fluctuates every hour. Additionally, it has been observed that the consumption pattern differs significantly on weak and regular days. Consequently, this problem is taken into account when creating the water heater

model. The following list illustrates the water heater's operating limits:

$$T_{wh}(t) = T_{wh}(t-1) + \nu_{wh}(T_{cold} - T_{hot}) + [\varphi O_i(k) - V_{cold}\omega_{wh}] \quad (30)$$

The internal temperature of the water heater is influenced by its ON/OFF status, usage habits, and the water's temperature at a specific interval (t) throughout the last hour.

2.7.3. Laundry machine, clothes dryer, and dishwasher

The following are the limitations on how the dishwasher, washing machine, and clothes dryer can operate:

$$\sum_{t=\tau_j} O_i(t) = OP_i^max, \forall t \in \tau_i \quad (31)$$

The total timeslots in a day that the devices must function in accordance with end-user preference are given by equation (31). During the modeling process, other limitations are considered, like the maximum consecutive operating duration and the need to coordinate the washing machine and fabric drier to avoid their starting simultaneously. The drying machine will start up after the washing machine has completed its cycle. Equation (32) confirms that the device will subsequently work to control the second type of appliances, which are referred to as uninterruptible appliances:

$$\sum_{xa} e_i(t) \cdot e_{i,t+1} \cdot e_{i,t+2} \cdot e^t + (\tau - 1) \geq 1 \quad (32)$$

$$S_{dryer} + S_{washer} \leq 1 \quad \forall t \in \tau \quad (33)$$

$$F_{i1} \geq F_{i2} + \tau_i \quad (34)$$

The textile dryer and washing machine cannot operate simultaneously, according to equation (33).

2.7.4. PAR decrease

Reducing the PAR allows us to achieve one of our primary objectives, which is to guarantee grid stability. The following is a mathematical expression for it [94]:

$$O_3 = min\ (PAR) \quad (35)$$

The PAR can be expressed formally as:

$$PAR = \frac{max\left(E\,Lood^{\,sch\ /\ unsch\ ^N}\right)^2}{\left(avg\left(ELood^{sch/unsch}\right)\right)^2} \quad (36)$$

where $E\,\text{Lood}^{\,sch^N} = \{E\,\text{Lood}^{\,sch^1}; E\,\text{Lood}^{\,sch^2}; E\,\text{Lood}^{\,sch^3}; \ldots; E\,\text{Lood}^{\,sch^{24}}\}$ is a list of the scheduled and unscheduled electrical load profiles for each hour is maintained in $E\,\text{Lood}^{\,unsch^N} = \left\{E\,\text{Lood}^{\,unsch^1}; E\,\text{Lood}^{\,unsch^2}; E\,\text{Lood}^{\,unsch^3}; \ldots; E\,\text{Lood}^{\,unsch^{24}}\right\}$.

2.7.5. Making users as comfortable as possible

Customers require some leeway in scheduling Smart Urban Buildings appliances in real-world situations. They ought to be able to ask for the scheduling of other appliances to accommodate their demands and turn off any equipment that they don't need. This rescheduling results in a somewhat shorter wait time for the user to turn on the required equipment. When an appliance is rescheduled on demand, the waiting time is zero, regardless of the user's previous demand time. Maximizing consumer comfort is our aim, and it can be expressed mathematically as:

$$O_4 = min\ (Comfort) \quad (37)$$

Coordination between the two parties ensures comfort when the user asks real-time rescheduling from $App_\uparrow^\alpha$ and the scheduler is interrupted Î to turn off an appliance. In formal words, this may be expressed as:

$$App^\alpha = \begin{cases} 1, if\ \widehat{I}, \\ 0, otherwise \end{cases} \quad (38)$$

where App^α represents an appliance that the user has turned on due to a run-time interruption. On the other hand, $App_\uparrow^\alpha \subseteq App$ is the list of appliances that the user wishes to change in real time. The scheduler will determine whether the operational time interval (O_{time}^{int}) and the available time interval ($Aval_{time}^{int}$) are compatible before turning on an appliance.

The waiting time $App_{W_t}^d$ and user comfort are inversely correlated. The mathematical expression for this relationship is as follows:

$$Comfort \propto \frac{1}{App_{W_t}^d} \quad (39)$$

where the symbol for an appliance's waiting time is $App_{W_t}^d$. The duration of an appliance's processing will be the basis for calculating user comfort in this thesis. It is calculated as:

$$App_{W_t}^d = \Delta\left(App_{Dmd}^d(\ hour\ ), App_{Sch}^d(\ hour\ )\right), Such\ that\ W_t \leq 24\ hour \quad (40)$$

The waiting time of the appliance $App_{W_t}^d$ should be less than 24 h. The constraint helps in ensuring that the desired appliance will be scheduled at least once within 24 h time domain.

3. Grasshopper optimization algorithm (GOA)

In natural environments, grasshopper swarms are modeled by the GOA. The following is a mathematical expression for this grasshopper swarm behavior [95].

$$P_i = SO_i + GRE_i + W_i \quad (41)$$

where P_i stands for the grasshoppers' location, SO_i for their social interaction force, GRE_i for their gravitational force, and W_i for their wind advection. Keep in mind that a random distribution of search agents throughout search space is necessary for all metaheuristic algorithms. The GOA algorithm's random behavior is provided by rewriting equation (41) as follows:

$$P_i = r_1 SO_i + r_2 GRE_i + r_3 W_i \quad (42)$$

This indicates that the random integers inside [0, 1] are r_1, r_2 and r_3. The force of social contact is the main search factor that the GOA algorithm found:

$$SO_i = \sum_{\substack{j=1; \\ j \neq i}}^{N} s(d_{ij})\widehat{d_{ij}} \quad (43)$$

When the following definitions apply: N is number of grasshoppers; d_{ij} is Euclidean distance between the i^{th} and j^{th} grasshoppers;

$$d_{ij} = |P_j - P_i| \quad (44)$$

Additionally, the method outlined below can be used to obtain $\widehat{d_{ij}}$, which represents a single vector from i^{th} to the j^{th} grasshoppers:

$$\widehat{d_{ij}} = \frac{(P_j - P_i)}{|P_j - P_i|} \quad (45)$$

As seen below, s represents a function that explains the strength of social forces:

$$s = fexp\left(-\frac{r}{l}\right) - exp(-r) \quad (46)$$

where the numbers l and f stand for the length scales of lustfulness and

attraction. In their social interactions, grasshoppers employ two different sorts of forces: attraction and repulsion. Repulsion takes place between [0, 2.079], while attraction rises between [2.079, 4] and likewise regularly falls. The range in which the distance is measured is [0,15]. The region is in its comfort zone when the distance is precisely 2.079, which indicates that no force is operating on it. For f and l, the recommended values are 0.5 and 1.5, respectively.

The definition of i^{th} grasshoppers' GRE_i (gravity force) can be expressed as follows;

$$GRE_i = -g\widehat{e_g} \tag{47}$$

where the earth's center is indicated by gravitational constant, $\widehat{e_g}$, and unity vector in direction of g. Wind advection of i^{th} grasshoppers, W_i, can be computed as follows:

$$W_i = u\widehat{e_w} \tag{48}$$

where the wind direction and direction are represented, respectively, by drift constant (u) and unity vector $\widehat{e_w}$. By altering the values of the previously mentioned components (i.e., SO_i; GRE_i; W_i), equation (41) can be represented as follows:

$$P_i = \sum_{\substack{j=1 \\ j\neq i}}^{N} s\left(\left|P_j - P_i\right|\right)\frac{(P_j - P_i)}{\left|P_j - P_i\right|} - g\widehat{e_g} + u\widehat{e_w} \tag{49}$$

It should be highlighted that because the grasshopper swarm does not converge to a single site, Equation (48) is unable to directly solve the optimization problem. In order to find the best solution to the issues raised by equation, a revised version of equation (50) is taken into consideration.

$$P_i^d = c\left(\sum_{\substack{j=1 \\ j\neq i}}^{N} c\frac{ub_d - lb_d}{2} s\left(\left|P_j^d - P_i^d\right|\right)\frac{(P_j - P_i)}{\left|P_j - P_i\right|}\right) + \widehat{T_d} \tag{50}$$

where the variables ub_d and lb_d represent the upper and lower bounds inside the d^{th} dimension. T_d represents the d^{th} dimension goal (best solution identified). Parameter c moves swarm closer to target.

The GOA algorithm's initial adjusting parameter, the reduction coefficient, must be lowered in accordance with the number of iterations. It is updated with the following formula.

$$c = c_{max} - t\frac{c_{max} - c_{min}}{t_{max}} \tag{51}$$

where maximum and minimum coefficient values of c are denoted by the variables c_{max} and c_{min}, respectively. The current and maximum iterations are represented by the symbols t and tmax, respectively. The values of c_{min} and c_{max} in this investigation are 10^{-5} and 1, respectively. Algorithm 1 shows the pseudocode for GOA.

Algorithm 1. **Grasshopper optimization algorithm**

Start: input, GOA parameters
Initialize: the swarm of grasshoppers randomly
Initialize: C_{min}, C_{max}, and maximum number of ittrations t_{max}
Evaluate: the fitness of each grasshopper $f(P_i)$
T = the best solution
while $(t < t_{max})Do$
update: C
for $i = 1,2 \ldots, n$ Do
for $j = 1{:}1{:}N$ Do
Normalize: the distance among grasshoppers
update the present position of the grasshopper
fetch the present grasshopper if it drives out the limits
end for
update T if the present solution is better than the previuse optimum solution
$t \leftarrow t + 1$
end while
output: return T = optimum soluion
end

3.1. An optimal load-shedding strategy derived from the GOA algorithm

The GOA is utilized in islanded case study system to determine best load-shedding strategy and MATPOWER power flow. To implement the suggested load-shedding method, the following protocols are used.

1) System input parameters: system parameters (such as load, line, and generator data) are provided to the algorithm.
2) Particle initialization and GOA parameter setting determine GOA parameters by entering number of repeats, degree of attraction, and the shirking factor parameter (*cmin*, *cmax*). The initial population size is generated at random. Proceed with stages 3–14 of the method, setting iteration = 0.3.
3) Configure the loop $t \leftarrow t + 1$.
4) Used MATPOWER power flow to compute complete voltage stability margin system and obtain the voltage deviation and power loss.
5) Fitness evaluation: Fitness function of every particle is evaluated.
6) Set this grasshopper on top here.
7) Adjust the variable c.
8) Ensure that the spacing between the grasshoppers is consistent.
9) Adjust the position P_i^d of the existing search agent.
10) To calculate voltage stability margin system overall and to calculate power loss and voltage deviation using MATPOWER power flow.
11) Each particle's fitness function is assessed.
12) If a better solution exists, update the location $\widehat{T_d}$ using the fitness function.
13) Stop criteria: save the best answer if the predetermined maximum iteration is reached; if not, proceed to step 3.

The flowchart for optimizing load shedding in the islanded system by implementing the GOA algorithm is depicted in Fig. 2.

4. Sine cosine algorithm (SCA)

A set of arbitrary solutions is frequently used at the start of the

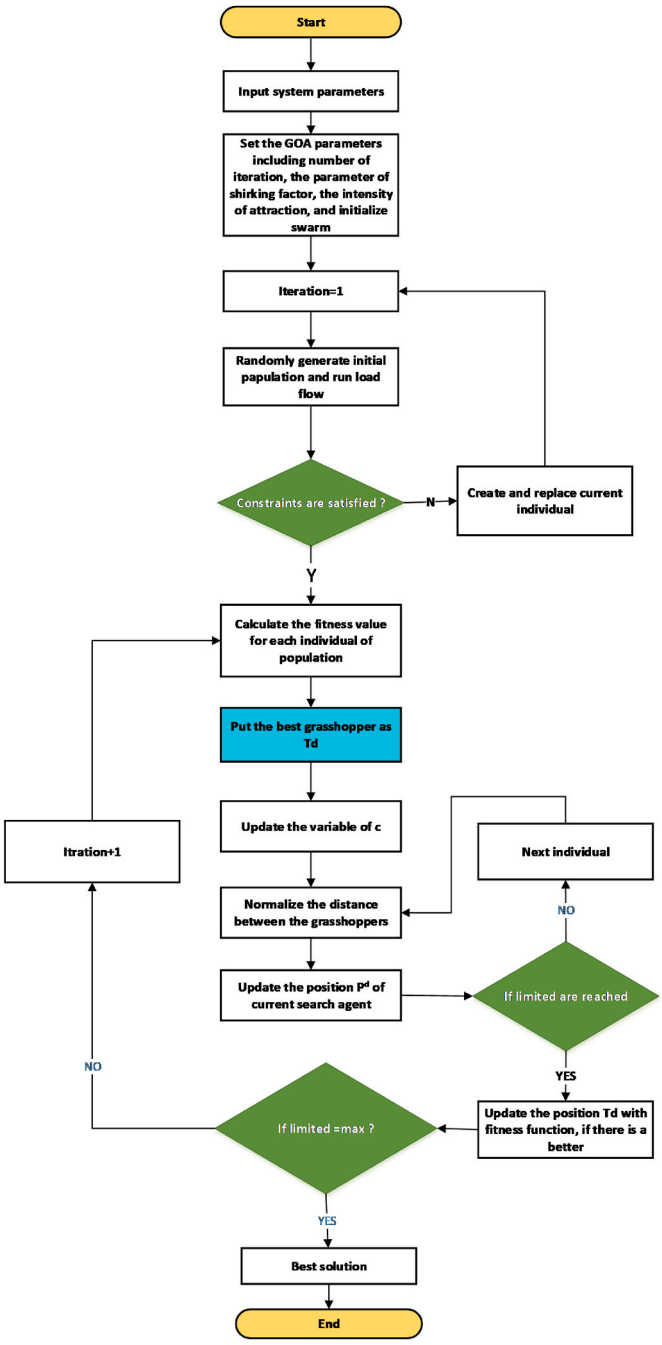

Fig. 2. The GOA flowchart for optimizing islanding operations, or load shedding.

optimization process in population-based optimization techniques. An optimization strategy's core consists of a set of rules that are used to improve this random set during its periodic evaluation by an objective function. Because population-based optimization techniques look for optima of optimization problems in a stochastically manner, there is no guarantee that a solution will be found in a single run of these techniques. But when there are enough random solutions and optimization steps (iterations), the chance of finding the global optimum increases. Different approaches are used in the field of stochastic population-based optimization, but they all split the optimization procedure into two stages: exploitation and exploration. An optimization method in the first phase connects the random solutions in the set of solutions with a high rate of unpredictability abruptly to find the interesting regions of the search space. But compared to the exploration phase, there are a lot less random fluctuations during the exploitation phase, and random solutions gradually alter during this stage. The position update equations shown below are proposed for both sections of this work [96]:

$$X_i^{t+1} = X_i^t + r_1 \times \sin(r_2) \times \left| r_3 P_i^t - X_i^t \right| \tag{52}$$

$$X_i^{t+1} = X_i^t + r_1 \times \cos(r_2) \times \left| r_3 P_i^t - X_{ii}^t \right| \tag{53}$$

where $r_1/r_2/r_3$ are random integers, P_i is the destination point's location in the $i-th$ dimension, and X_i^t is the current solution's position in the i-th dimension at the t-th iteration. The following is the result of combining these two equations:

$$X_i^{t+1} = \begin{cases} X_i^t + r_1 \times \sin(r_2) \times \left| r_3 P_i^t - X_i^t \right|, & r_4 < 0.5 \\ X_i^t + r_1 \times \cos(r_2) \times \left| r_3 P_i^t - X_{ii}^t \right|, & r_4 \geq 0.5 \end{cases} \tag{54}$$

where r_4 in [0,1] is a random number.

There are four primary parameters in SCA, as the aforementioned equations demonstrate: r_1, r_2, r_3, and r_4. The region (or movement direction) of the next location is determined by the parameter r_1, and it might be outside the destination or inside the area between the solution and it. How far the movement should be in the direction of or away from the target is determined by the parameter r_2. The destination's impact on defining the distance can be stochastically emphasized $(r_3 > 1)$ or deemphasized $(r_3 < 1)$ by adjusting the parameter r_3. Lastly, in Eq. (53), the parameter r_4 alternates equally between the sine and cosine components.

The Sine Cosine Algorithm (SCA) is the term given to this algorithm since it uses both sine and cosine in its formulation. Fig. 3 shows how Sine and Cosine affect Equations (52) and (53). This image illustrates how a gap between two solutions in the search space is defined by the suggested equations. Note that although Fig. 3 shows a two-dimensional model, this equation can be extended to higher dimensions. One answer can be repositioned around another solution using the sine and cosine functions' cyclic pattern. This can ensure that the space defined between two solutions is exploited. The solutions should also be able to search outside the space between their respective targets in order to fully explore the search space. As seen in Fig. 4, this can be accomplished by adjusting the sine and cosine functions' ranges.

Fig. 5 shows a conceptual model of the impacts of the sine and cosine functions with a range of $[-2,2]$. This figure illustrates how a solution must update its position outside or inside the space between itself and another solution in order to change the range of the sine and cosine functions. To determine the random location, either inside or outside of $[0,2\pi]$, define a random number for r_2 in Eq. (54). As a result, this process ensures that the search space is explored and utilized, respectively.

In order to locate the most promising areas of the search space and ultimately converge to the global optimum, an algorithm must be able to strike a balance between exploration and exploitation. The range of sine and cosine in Eqs. (52)–(54) is adjusted adaptively using the following equation to strike a balance between exploration and exploitation:

$$r_1 = a - t\frac{a}{T} \tag{55}$$

where an is a constant, T is the maximum number of iterations, and t is the current iteration.

The range of the sine and cosine functions is reduced by this equation throughout the number of repetitions, as Fig. 6 illustrates. From Figs. 5 and 6, one may deduce that the SCA algorithm searches the space when the sine and cosine function ranges are in (1,2] and [−2,-1). But when the ranges fall within the interval [−1,1], this technique takes advantage of the search space.

Subsequently, the algorithm stores the optimal solutions found thus far, designates it as the destination, and modifies the remaining solutions in light of it. As the iteration counter rises, the sine and cosine function ranges are updated to highlight searching the whole search

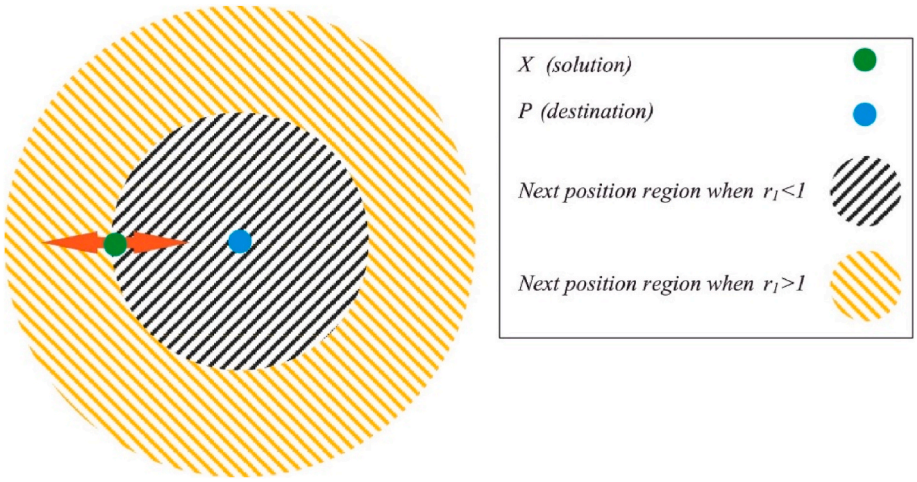

Fig. 3. The next location is affected by the sine and cosine in equations (3.1) and (3.2).

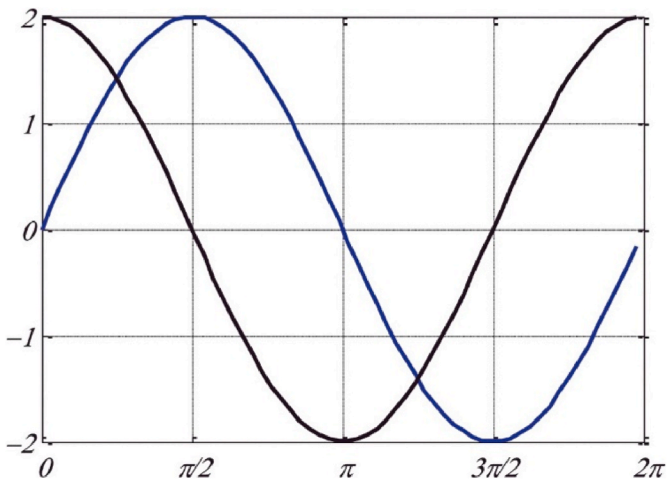

Fig. 4. The range of sine and cosine is [−2,2].

space. When the iteration counter exceeds the maximum number of iterations by default, the SCA algorithm ends the optimization process. Any other termination condition, such as the precision of the achieved global optimum or the maximum number of function evaluations, can be taken into consideration, nevertheless.

4.1. Improved sine cosine algorithm (ISCA) framework

Similar to the traditional SCA, the suggested ISCA begins with an identical set of uniformly distributed solutions (referred to as the population) inside the search space in order to evaluate how well the search procedure works in ISCA. The population of solutions is initialized, and then the process of looking for the problem's optima begins. The following is the updated search equation that ISCA introduced [97]:

$$v_{i,t+1} = \begin{cases} x_{i,t} + A\sin(r_1)\left|Cx_{i,pBest} - x_{i,t}\right| + r_2\left(x_{\text{Best}} - x_{i,t}\right)^{\text{Social Component}} & ifr \\ < 0.5x_{i,t} + \underbrace{A\cos(r_1)\left|Cx_{i,pBest} - x_{i,t}\right|}_{\text{Cognitive Component}} + \underbrace{r_2\left(x_{\text{Best}} - x_{i,t}\right)}_{\text{Social Component}} & O.W \end{cases} \tag{56}$$

where r_2 is a uniformly distributed random number between 0 and 1, $x_{i,t}$ is the solution at iteration t, $x_{i,pBest}$ is the best position within the population of solutions, and $x_{i,pBest}$ is the current best position acquired thus far of the solution. As in traditional SCA, all other parameters, including A, r_1, C, and r, are the same.

The search process's cognitive component is contributed by the second term on the right in Eq. (56) and its social component is contributed by the third term. Conducting both local and worldwide searches when conducting the search has the advantage of addressing these two factors. By merging the directions along the best possible path for both the population and the solution, the cognitive and social components provide the current solution an effective and hopeful direction.

When the search area supplied by the coefficient A is sufficiently large, there is a possibility that the solution updated with the aid of Equation (56) will deviate from the present state of the solution.

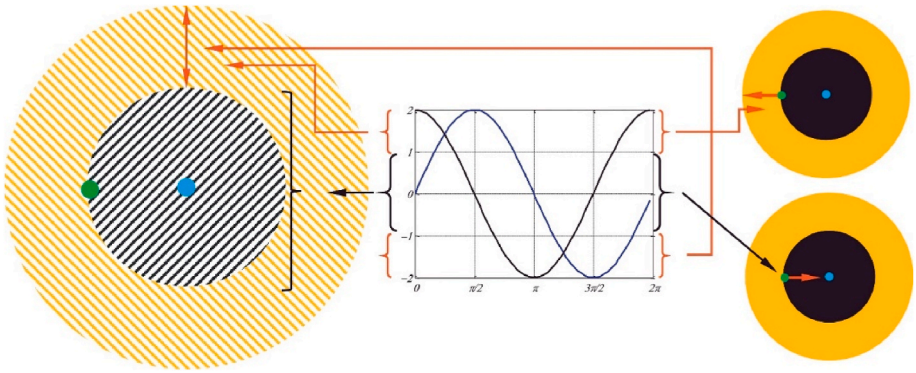

Fig. 5. A solution can go around (within the space between them) or beyond (outside the space between them) the target when using sine and cosine with ranges in [−2,2].

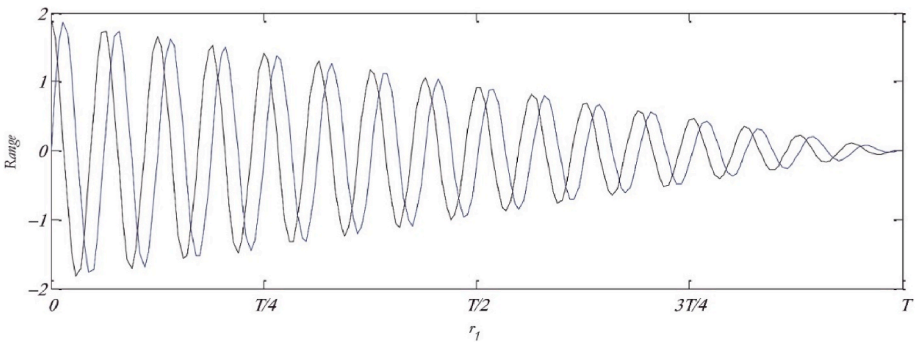

Fig. 6. Pattern of decreasing sine and cosine (a = 3).

Therefore, the updated solution $v_{i,t+1}$ is crossed with the current best solution $x_{i,pBest}$ of solution x_i in order to deal with such a circumstance and to integrate the own best aspects of a solution.

Following the crossover mechanism, a greedy selection process is carried out between the found solution (ui) and the current best solution $x_{i,pBest}$. This process maintains the equilibrium between exploration and exploitation during the search phase. The flowchart in Fig. 7 provides a concise summary of all the steps mentioned above. Fig. 8: The suggested load shifting algorithm's flow chart.

5. Using probabilistic optimality to plan storage system capacity

The next subsections propose a two-stage strategy consisting of an outer optimal sizing phase and a nested dispatch optimization loop for the coordinated, system-level design and dispatch co-optimization of storage systems integrated into grid-connected MGs.

5.1. *When to use operational scheduling at its best*

In light of the day-ahead, local generation, load demand, and

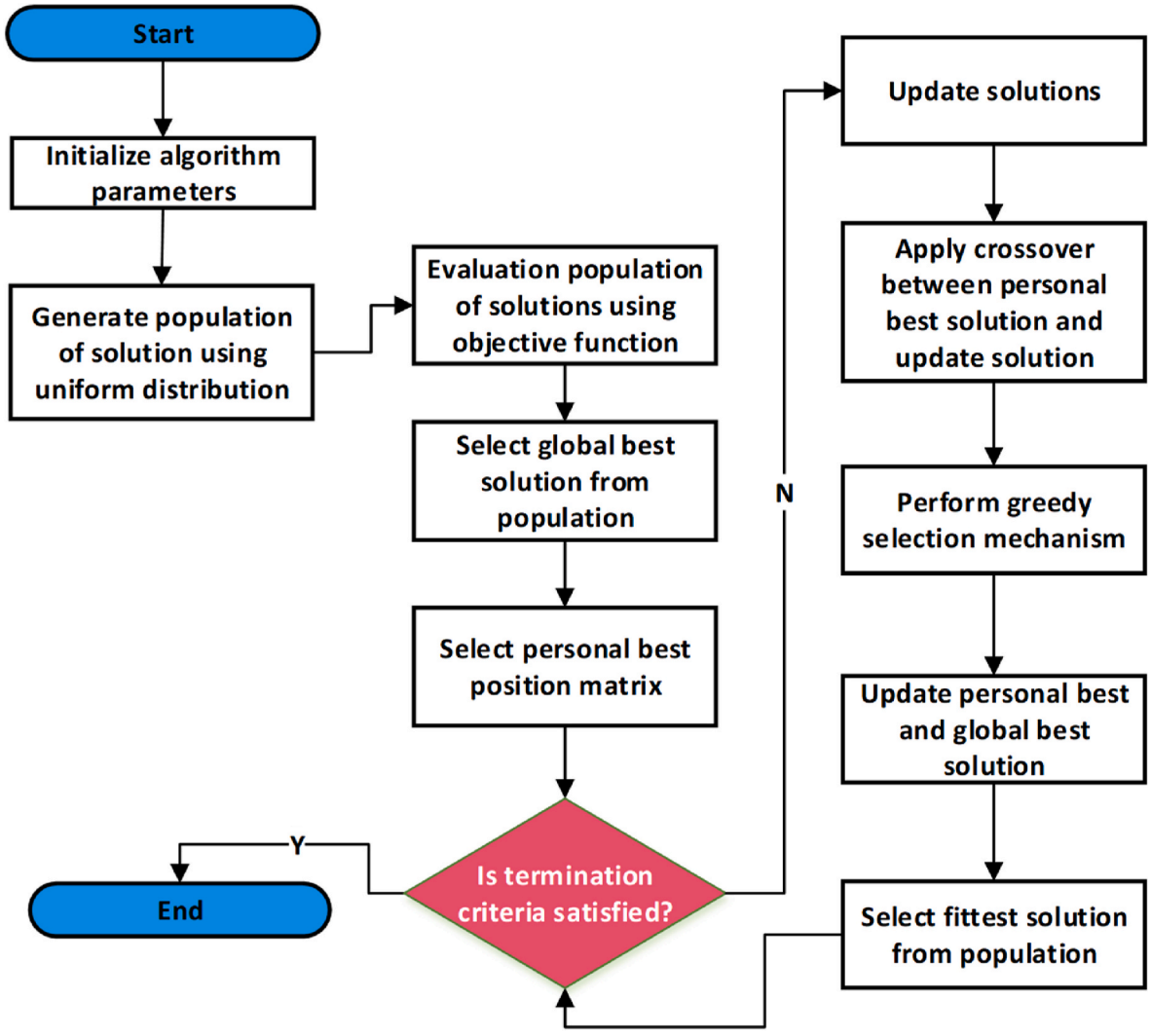

Fig. 7. An improved sine cosine algorithm (ISCA) flow chart is proposed.

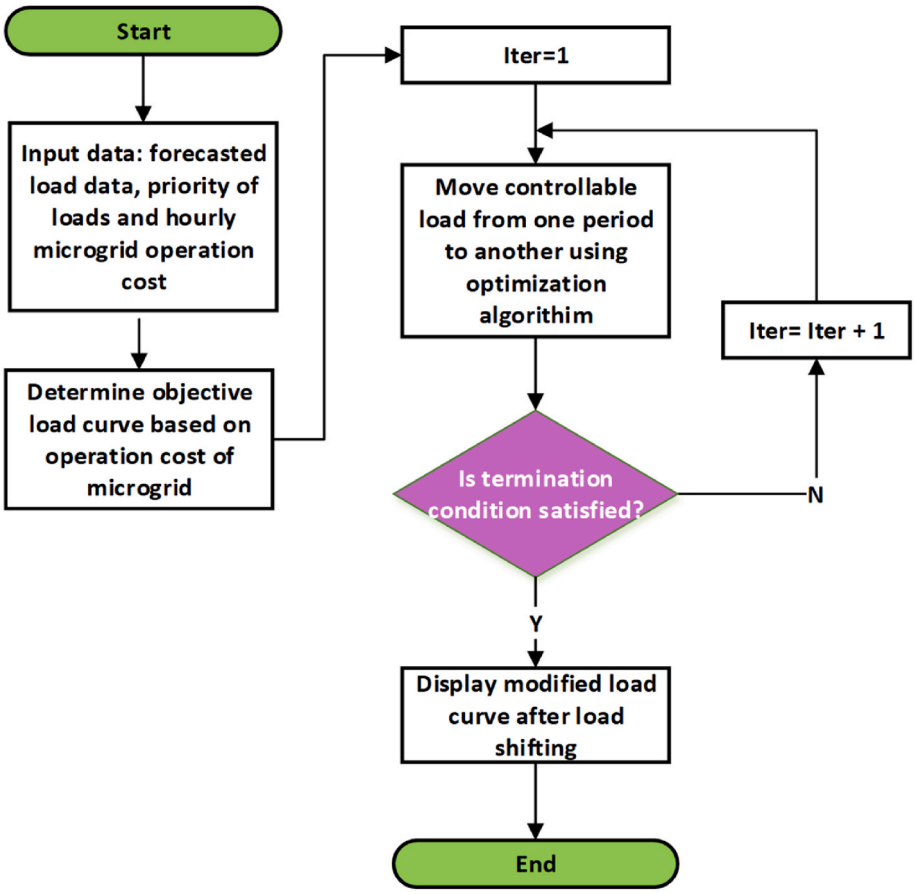

Fig. 8. Diagram illustrating the suggested load shifting algorithm.

wholesale energy pricing, the optimal time to charge and discharge the hybrid storage system was determined. This paragraph explains the hourly-basis rule-based operational planning approach that was devised. In order to optimally regulate the functioning of the hybrid storage system, the operational strategy is designed to use linear programming formulas, assuming that the wholesale pricing, local generation, and demand for the next 24 h will be accessible. It is interesting to note that the storage follows the widely accepted arbitrage idea of "dis-respectively discharging at a cheap cost". The following equations describe the day-ahead profit maximization problem in day-ahead energy management. Bold characters indicate 24-h column vectors [98].

$$maxPr = P_{ex}\, FiT^{T}\Delta t - P_{im}\pi^{T}\Delta t - 10^{-6}\| u\|_{1}, \tag{57}$$

Subject to:

$$P_{im} - P_{ex} = P_{L} - P_{RE} + P_{ch,B} - P_{dch,B} + P_{ch,SC} - P_{dch,SC} \tag{58}$$

$$E_{\frac{B}{SC}}(t) = E_{\frac{B}{SC}}(t-1)\cdot\left(1-\sigma_{\frac{B}{SC}}\cdot\Delta t\right) + \eta_{ch,\frac{B}{SC}}\cdot P_{ch,\frac{B}{SC}}(t)\cdot\Delta t - \frac{P_{dch,\frac{B}{SC}}(t)\cdot\Delta t}{\eta_{dch,\frac{B}{SC}}}\ \forall t \tag{59}$$

$$C^{min}_{\frac{B}{SC}} \le E_{\frac{B}{SC}}(t) \le C_{\frac{B}{SC}}(\ cycle\ )\forall t \tag{60}$$

$$0 \le P_{ch,\frac{B}{SC}}(t) \le u_{ch}(t)\cdot P^{max}_{ch,\frac{B}{SC}} \quad \forall t \tag{61}$$

$$0 \le P_{dch,\frac{B}{SC}}(t) \le u_{dch}(t)\cdot P^{max}_{dch,\frac{B}{SC}}\forall t \tag{62}$$

$$u_{ch}(t) + u_{dch}(t) = 0\forall t \tag{63}$$

$$0 \le P_{im}(t) \le u_{im}(t)\cdot\left(N_I\cdot P_{I,r} + P_{I,ins}\ \right)\ \forall t \tag{64}$$

$$0 \le P_{ex}(t) \le u_{ex}(t)\cdot\left(N_I\cdot P_{I,r} + P_{I,ins}\ \right)\forall t \tag{65}$$

$$u_{im}(t) + u_{ex}(t) \le 1\ \forall t \tag{66}$$

where P_{im} stands for imported power, P_{ex} for exported power, P_L for load power, P_{RE} for renewable energy generation, FiT for feed in tariff, and π for wholesale electricity price. Pr is the day − ahead profits′ 24 − hour vector. $P_{ch,B}$ and $P_{dch,B}$ indicate the battery bank's charging and discharging power, respectively, and $P_{ch,SC}$ and $P_{dch,SC}$ indicate the SC bank's charging and discharging power. Battery/SC bank's energy content is represented by $E_{\frac{B}{SC}}$, its self-discharge rate is represented by σB/SC, its charging and discharging efficiencies are indicated by $\eta_{ch,\frac{B}{SC}}$ and $\eta_{dch,\frac{B}{SC}}$, respectively, and its charging and discharging powers are represented by $P_{ch,\frac{B}{SC}}$ and $P_{dch,\frac{B}{SC}}$, respectively. $P^{max}_{ch,\frac{B}{SC}}$ and $P^{max}_{dch,\frac{B}{SC}}$, respectively, reflect the battery/SC bank's maximum power for charging and discharging. The binary variables u_{ch} and u_{dch} are used to make sure that charging and discharging don't happen simultaneously, and u_{im} and u_{ex} ensure that importing and exporting don't happen simultaneously. N_I is the optimal inverter size to be installed, $P_{I,r}$ is inverter's rated power to be installed, and $P_{I,\mathrm{ins}}$ is the inverter's capacity that is now installed

The energy content of the battery at each time step in Equation (58) is defined by the energy storage devices' charging and discharging power components, onsite renewable power generation, load power, imported and exported power, and overall power balance, as stated above. This establishes the power balance constraint. The last part of the

objective function, $10^{-6}\|u\|_1$, penalizes solutions involving unprofitable cycling in day-ahead operational scheduling optimization by considering net present cost (NPC) of storage deterioration brought on by cycling. L-1 norm of storage schedules serves as its foundation, and it can be found using the formula $\|u\|_1 = \sum_{t=t_1}^{t_1+24} \left(P_{ch,B}(t) + P_{dch,B}(t) + P_{ch,sc}(t) + P_{dch,SC}(t)\right)$. Additionally, note that Equation (16) establishes a lower bound on the energy stored in the battery bank, which is $1 - DOD_B) \times C_B(cycle)$, where DOD_B is the corresponding DOD of the battery. Additionally, the lowest limit on the energy content of the energy storage bank is set at zero because the EDLC SCs under consideration in this study may be constantly discharged to 100 % DOD without experiencing any long-term consequences. Additionally, by using two binary control variables, the constraint ensures that storage is not in both charging and discharging modes at the same time step. Furthermore, the maximum capacity of the bidirectional inverter—which encompasses both installed and newly added capacity—limits the quantity of electricity that may be exchanged with the grid.

5.2. The ideal stage of capacity planning

Using the ideas of net present cost (NPC) and net present value (NPV), an objective function is built to assess the economic worth of investing in energy storage systems. NPC linked to every recently installed part, such as the inverter and battery, can be acquired as:

$$NPC = N_c \times \left(CC + RC \times SPPW + \frac{O\&M}{CRF(ir, PL)} - SV\right) \tag{67}$$

$$SPPW = \sum_{i=1}^{N} \frac{1}{(1+ir)^{CL \times i}} \tag{68}$$

$$N = \begin{cases} \left\lfloor \frac{PL}{CL} \right\rfloor - 1 \ if\ PLmodCL = 0 \\ \left\lfloor \frac{PL}{CL} \right\rfloor \ if\ otherwise \end{cases} \tag{69}$$

$$CRF(ir, PL) = \frac{ir(1+ir)^{PL}}{(1+ir)^{PL} - 1} \tag{70}$$

$$SV = RC \times \frac{CL - \left(PL - CL \times \left\lfloor \frac{PL}{CL} \right\rfloor\right)}{CL} \tag{71}$$

where the notations CC, RC, and O&M stand for capital, replacement, and operation and maintenance expenses, and N_c is the optimum capacity of component c. The notations CC,RC, and $O\&M$ stand for capital, replacement, and operation and maintenance expenses, and N_c is optimum capacity of component c. CRF stands for capital recovery factor, and $SPPW$ is for single-payment present-worth factor, project lifespan (PL), component lifetime (CL), and interest rate (ir) are represented by the acronyms.

The cycle life of the storage components can easily be converted to calendar life using the following equation:

$$R_S = \frac{N_S \times Q_{life}}{Q_{thr}} \tag{72}$$

where Q_{life} and Q_{thr} stand for the storage component's lifetime and annual storage, respectively, and N_S is its ideal capacity. Additionally, the net present value (NPV) of total power exchanged with grid over project's lifetime can be calculated using the formula below.

$$NPV_{exch} = \sum_{i=1}^{PL} \frac{C_{exch}^{i}}{(1+ir)^{i}} \tag{73}$$

where C_{exch}^{i} , which may be derived as follows;

$$C_{exch} = \sum_{t=1}^{T} P_{im}(t) \cdot \pi(t) - P_{ex}(t) \cdot FiT \tag{74}$$

As a result, the optimal hybrid storage sizing problem's objective function is specified as:

$$minTNPC = NPC_B + NPC_I + NPV_{exch} + c \tag{75}$$

where NPV_{exch} is net present value of power exchanges, NPC_B, NPC_{SC}, and NPC_I stand for battery, NPV_{exch} for inverter, respectively. A penalty factor, c, is added to the objective function's returned value if any of the imposed constraints are broken.

5.2.1. Limitations

The following conditions must be met by the nested optimal dispatch optimization step: the restrictions on battery and SC bank energy content and charging/discharging power.

5.2.1.1. The store's initial energy limitations. To ensure an efficient feeding of the peaks that occur early in the 24-h scheduling period, the battery and SC banks are programmed to be full in the first iteration, as:

$$E_{B,SC}(0) = N_{\frac{B}{SC}} \cdot C_{\frac{B}{SC}}(0) \tag{76}$$

5.2.1.2. Limitations on in-store terminal energy. The energy contents of battery and SC banks at conclusion of operational analysis period must be equal to or higher than their beginning energy contents in order to provide balanced research:

$$E_{\frac{B}{SC}}(T) \geq E_{\frac{B}{SC}}(0) \tag{77}$$

5.2.1.3. The least amount of independence. A minimal self-sufficiency ratio (SSR), or the percentage of load satisfied by onsite distributed energy resources (DERs) during energy scheduling, is used to address the optimal sizing problem:

$$SSR \geq SSR^{min} \tag{78}$$

$$SSR = \frac{\sum_{t=1}^{T} P_L(t) - P_{im}(t)}{\sum_{t=1}^{T} P_L(t)} \tag{79}$$

where P_L is local load, P_{im} is imported power, and SSR^{min} is pre-defined minimum SSR imposed.

5.2.1.4. Constraints on energy resilience. The minimum autonomy hour of the energy storage system and the minimum grid outage survivability, which are respectively defined as the ratio of the storage size to the mean total annual load demand and the ratio of the storage size to the mean total annual net load demand (load minus local generation), are the two energy resilience constraints that the capacity planning optimization must meet:

$$AH_{\frac{B}{SC}} \geq AH_{\frac{B}{SC}}^{min} \tag{80}$$

$$AH_{\frac{B}{SC}} = \frac{\left(N_B \cdot P_{B,r} + N_{SC} \cdot P_{SC,r}\right)}{\frac{\left(\sum_{t=1}^{T} P_L(t)\right)}{T}} \tag{81}$$

$$GOS_{MG} \geq GOS_{MG}^{min} \tag{82}$$

$$GOS_{MG} = \frac{\left(N_B \cdot P_{B,r} + N_{SC} \cdot P_{SC,r}\right)}{\frac{\left(\sum_{t=1}^{T} P_L(t) - P_{RE,ins}(t)\right)}{T}} \tag{83}$$

where $P_{B,r}$ and $P_{SC,r}$ respectively denote the rated power of the battery and SC banks; T is the final time-step of the operational analysis period; $AH_{B/SC}^{min}$ is the minimum autonomy hour of the battery/SC imposed; GOS_{MG}^{min} is the minimum grid outage survivability imposed; and N_B and N_{SC} respectively denote the optimal capacity of the battery and SC banks.

5.2.1.5. Maximum power supply loss. A maximum loss of power supply probability (LPSP) reliability requirement must be satisfied by the outer design optimization problem's optimal solution:

$$LPSP \leq LPSP^{max} \tag{84}$$

$$LPSP = \frac{\sum_{t=1}^{T} \left(LPS(t) \times \Delta t\right)}{\sum_{t=1}^{T} \left(P_L(t) \times \Delta t\right)} \tag{85}$$

$$LPSP(t) = \begin{cases} P_L(t) - P_G(t) \text{ if } P_L(t) > P_G(t) \\ 0 \text{ if otherwise} \end{cases} \tag{86}$$

$$P_G(t) = P_{PV}(t) + P_{WT}(t) + P_{dch,B}(t) + P_{dch,SC}(t) + P_{im}(t) \quad \forall t \tag{87}$$

The total power available for supplying local loads via on-site generation, discharging storage components, and importing power from the grid is measured by the auxiliary variable PG. The amount of power supply loss is represented by LPS. where $LPSP^{max}$ represents the highest power supply probability loss that is enforced.

5.2.1.6. Limits on decision variables. The non-negative choice variables are also upper constrained due to computer cost considerations, which helps to limit the search space:

$$0 \leq N_B \leq N_B^{max} \tag{88}$$

$$0 \leq N_I \leq N_I^{max} \tag{89}$$

$$0 \leq N_T \leq N_T^{max} \tag{90}$$

where N_B^{max}, N_I^{max}, and N_T^{max} stand for battery, inverter, and transformer's respective maximum capacities.

5.2.2. A technique for optimization

The moth-flame optimization algorithm (MFOA), a cutting-edge metaheuristic optimizer, is used to optimize the objective function [99]. MFOA emulates the swarm behavior of moths around flames to maximize a problem-solving method. In particular, equations are used to update moth positions in design space.

$$M_i = S\left(M_i, F_j\right) \tag{91}$$

$$S\left(M_i, F_j\right) = D_{ij} e^{bt} \cos(2\pi r) + F_j \tag{92}$$

$$D_{ij} = \left|F_j - M_i\right| \tag{93}$$

where D_{ij} is the Euclidean distance between moth i and flame j, $S\left(M_i, F_j\right)$ is the spiral function of moth i and flame j, and b is a constant that defines the shape of the logarithmic spiral.

5.3. Synopsis of the proposed two-phase energy storage system design paradigm

The two-stage stochastic solution approach based on meta-heuristics created for hybrid storage capacity optimization model is shown in Figs. 9 and 10. As seen in Fig. 9, the issue is split into two parts: an outer loop storage sizing problem and a nested optimal energy scheduling challenge. A vector of choice variables (here-and-now design variables) is provided to an inner loop optimal scheduling problem by an outer loop optimal sizing problem.

Wait-and-see options result from the optimal scheduling problem, whose solution considers choice factors as parameters. Every 24 h during the baseline year, the optimal scheduling problem is resolved, and the solutions to the optimal design problem are given in order to evaluate the fitness of each design (total NPC).

The operational planning model is expressed as a linear programming issue and is solved using the built-in MATLAB linear programming optimizer, whilst the long-term investment planning problem is handled by the MFOA. Each search agent in the MFOA is represented by a vector that shows the investment decision variables to be made throughout the study period. Every iteration, the MFOA creates an investment portfolio with the best DER asset sizes and cost-effective dispatch schedules, subject to operational limitations. The associated indices are then computed by feeding the optimized variables into the evaluation blocks for the grid outage survivability, energy storage system autonomy hour, LPSP, and SSR. Once maximum number of iterations is achieved, MFOA's search and selection procedure is subject to a set of planning-level limitations that are established based on the previously specified indices.

6. Results and analysis

In this section, the suggested SUBs simulation results are displayed. This program's main objectives are to minimize PAR, reduce the cost of using electricity, and improve User Comfort (UC) by shortening wait times. It has been claimed in this research that a 24-h schedule strikes a good balance between these goals. The outcomes of Unscheduled, Grasshopper Optimization Algorithm (GOA), Improved sine cosine algorithm (ISCA) are compared using RTP in order to verify the accuracy of the system.

Fig. 11 shows the photovoltaics power curve, Fig. 12 shows the wind turbine power curve.

6.1. Pricing tariffs

The retail company's expenditure has been used to compute the overall electricity cost. In order to do this, a variety of flexible pricing techniques are employed in an effort to reduce the overall cost of energy that consumers use, hence improving the PAR and protecting the UC. When utilizing electric gadgets, researchers use a range of pricing strategies to persuade people to switch from expensive to inexpensive moments. According to the RTP costing view, the price of the signals varies in accordance with different instances, but the expense is constant for each session (based on the per-hour consumption of power). The appropriate steps must be followed whenever an energy provider records prices that are too high compared to the market or encounters an emergency. Fig. 13 depicts the price tariffs in terms of RTP.

6.2. Load consumption

This section looked at the power consumption of several methods, including as the proposed ISCA algorithm, unscheduled, and GOA. Fig. 14 contrasts these methods.

6.3. RTP based pricing

When compared to other methods, the suggested hybrid ISCA strategy likewise shows an incredibly successful energy usage plan. The cost of electricity when taking RTP into account is shown in Fig. 15. . Considering RTP, the total cost of power is displayed in Fig. 16. One way

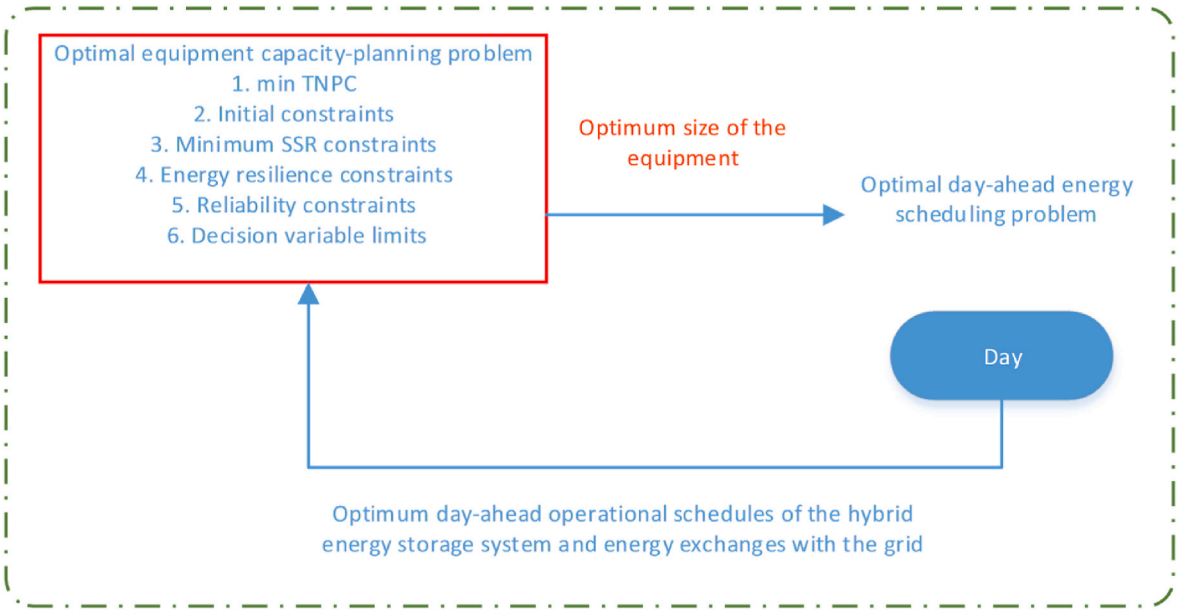

Fig. 9. Layered optimum scheduling issue with optimal stochastic storage.

to achieve this is through the use of Demand Side Management (DSM), an essential component of both micro-grid and Smart Grid technology. Maintaining client confidence and enforcing strict regulations are two ways to achieve DSM. Most of the DS Initiatives that are the subject of this paper are designed to help Smart Urban Buildings better manage their power plan. The suggested framework employed in this study is based on Real-Time-Price (RTP) payment procedures. Two operational instances (24 h) are considered in order to evaluate customer demands and conduct in accordance with the recommended course of action. Simulation findings show that the proposed method arranges the devices in the best possible way, minimizing energy consumption without compromising user comfort (UC). Customers may have to pay extra for the highest level of comfort due to waiting times for gadgets. Consequently, the suggested model's superiority is greater.

6.4. RTP based PAR

The PAR curves for RTP are displayed in Fig. 17, which suggests that the suggested method outperforms alternative approaches in terms of results.

6.5. Waiting time

UC is established by the length of time a user waits for gadgets. Therefore, there is always a trade-off between lowering PAR and EC or lowering power usage and device wait times. Due of gadget waiting periods, customers may pay more for the greatest level of comfort. In an unforeseen circumstance, there is almost never any waiting time because equipment is activated based on user comfort. In Fig. 18, the waiting duration for RTP is displayed.

The proposed system is evaluated by comparing it with the Grasshopper Optimization Algorithm (GOA) and unscheduled cases. Without applying an optimization algorithm, the total electricity cost, carbon emission, PAR and waiting time are equal to 1703.576 ID, 34.16664 (kW), and 413.5864s respectively for RTP. While, after applying GOA, the total electricity cost, carbon emission, PAR and waiting time are improved to 1469.72 ID, 21.17 (kW), and 355.772s respectively for RTP. While, after applying the ISCA Improves the total electricity cost, PAR, and waiting time by 1206.748 ID, 16.5648 (kW), and 268.525384s respectively. According to the results, the created ISCA algorithm performed better than the unscheduled case and GOA scheduling situations in terms of the stated objectives and was advantageous to both utilities and consumers.

Where after applying GOA, the total electricity cost, PAR, and waiting time are improved to 13.72 %, 38.00 %, and 13.97 % respectively. And after applying proposed method, the total electricity cost, PAR, and waiting time are improved to 29.16 %, 51.51 %, and 35.07 % respectively.

7. Conclusion

In this study, an Improved Sine Cosine Algorithm (ISCA)-based Smart Urban Buildings (SUBs) architecture is proposed to minimize total daily electricity costs, minimize peak to average ratio (PAR), and minimize the waiting time in SUBs by facilitating optimal DR and self-consumption. The proposed algorithm schedules tasks of all types of manageable electrical loads. The proposed system is evaluated by comparing it with the Grasshopper Optimization Algorithm (GOA) and unscheduled cases. Without applying an optimization algorithm, the total electricity cost, carbon emission, PAR and waiting time are equal to 1703.576 ID, 34.16664 (kW), and 413.5864s respectively for RTP. While, after applying GOA, the total electricity cost, carbon emission, PAR and waiting time are improved to 1469.72 ID, 21.17 (kW), and 355.772s respectively for RTP. While, after applying the ISCA Improves the total electricity cost, PAR, and waiting time by 1206.748 ID, 16.5648 (kW), and 268.525384s respectively. According to the results, the created ISCA algorithm performed better than the unscheduled case and GOA scheduling situations in terms of the stated objectives and was advantageous to both utilities and consumers.

Where after applying GOA, the total electricity cost, PAR, and waiting time are improved to 13.72 %, 38.00 %, and 13.97 % respectively. And after applying proposed method, the total electricity cost, PAR, and waiting time are improved to 29.16 %, 51.51 %, and 35.07 % respectively.

The life-cycle cost of the SUBs can be considerably decreased by up to 25 % by deploying energy storage systems incorporated into grid-connected MGs using an efficient scheduling design framework with 24-h look-ahead periods. A regulation-based energy dispatch strategy based on greed is the antithesis of this. By maximizing the utilization of the energy resources that are currently available, this technique reduces costs.

Future works will be conducted by introducing energy storage

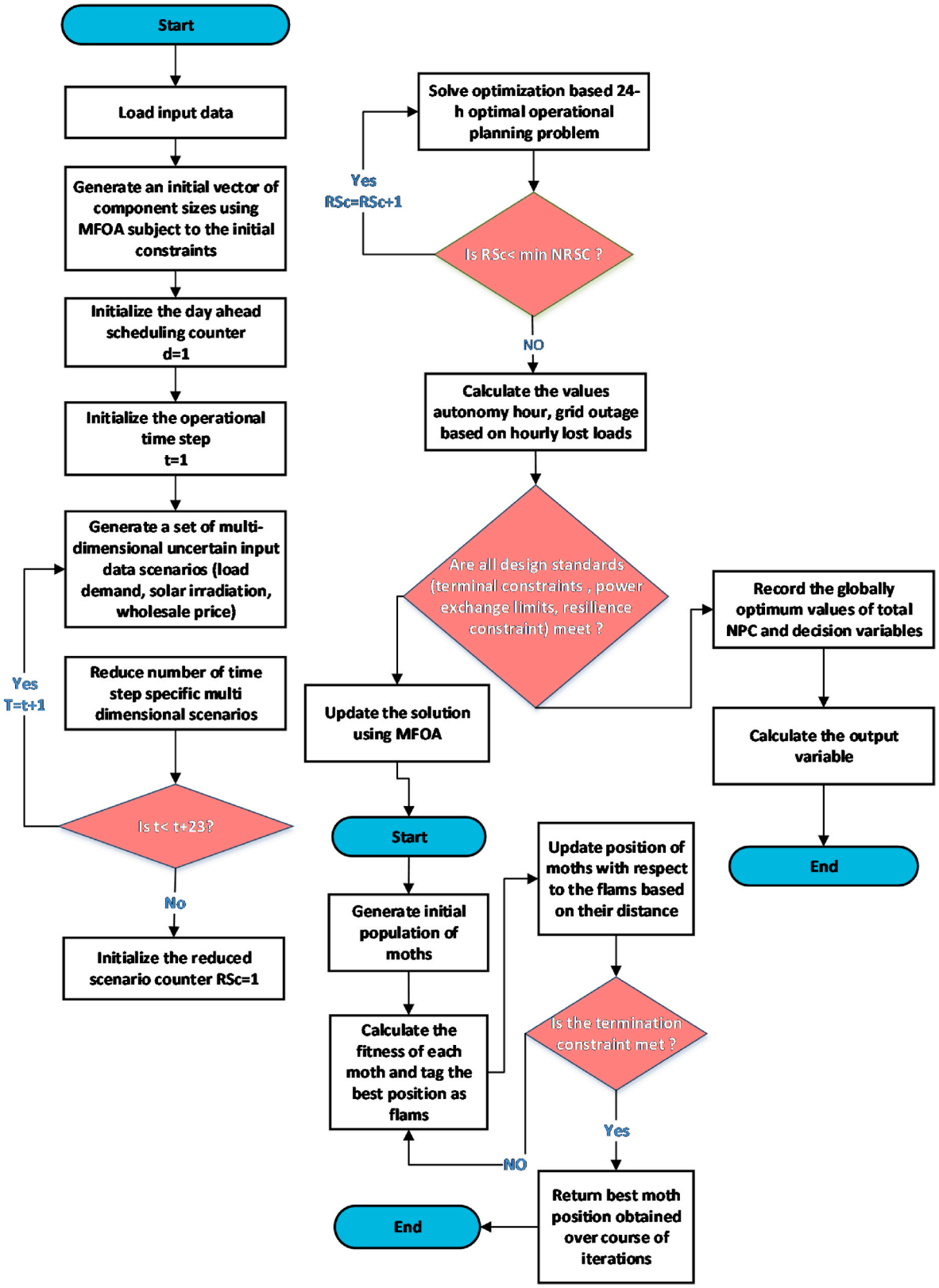

Fig. 10. Stochastic energy storage system planning framework.

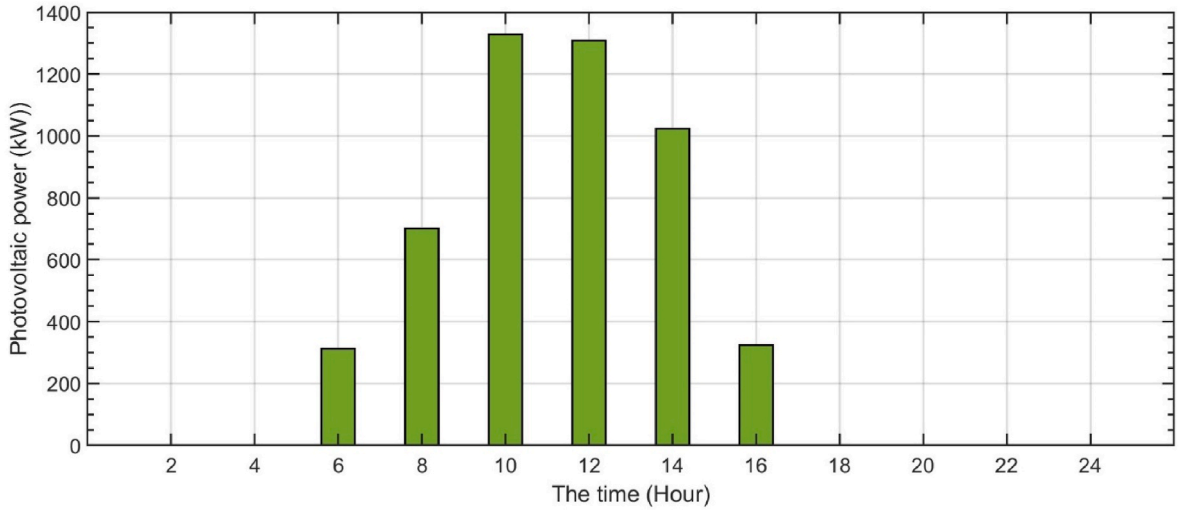

Fig. 11. Photovoltaics power curve.

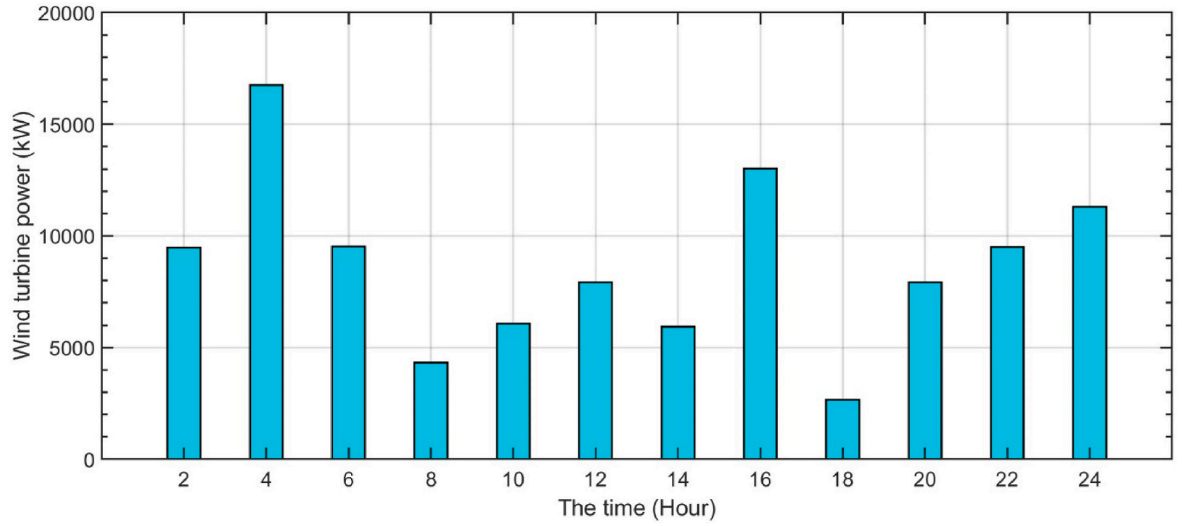

Fig. 12. Wind turbine power curve.

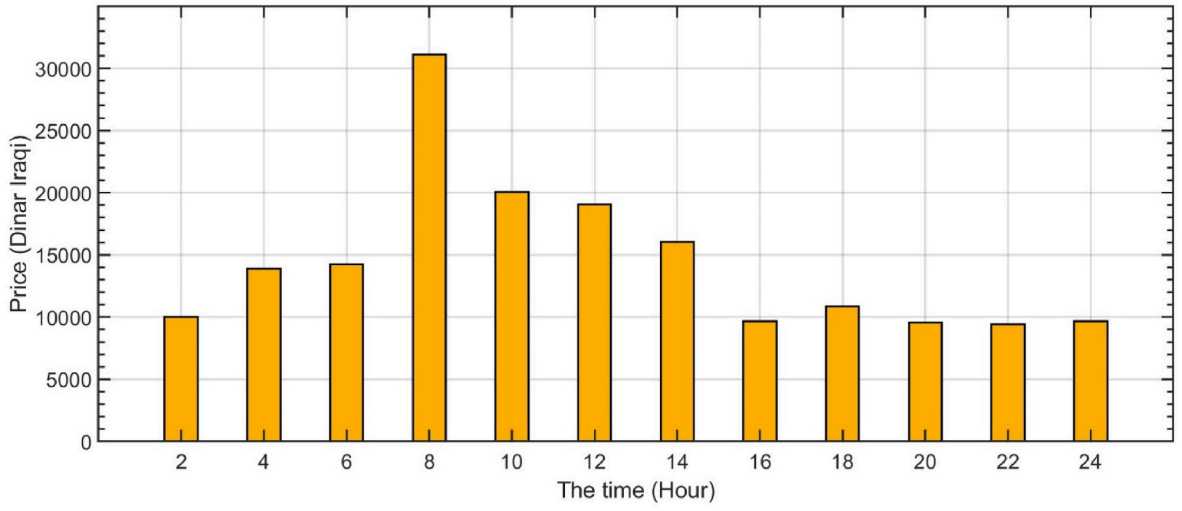

Fig. 13. Tariffs on prices expressed in RTP.

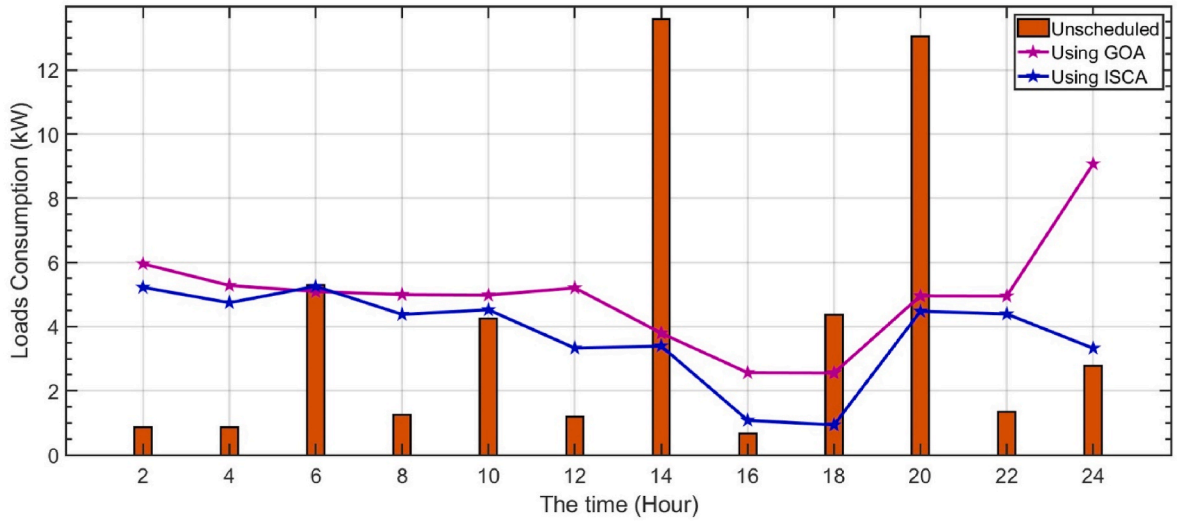

Fig. 14. Consumption of energy.

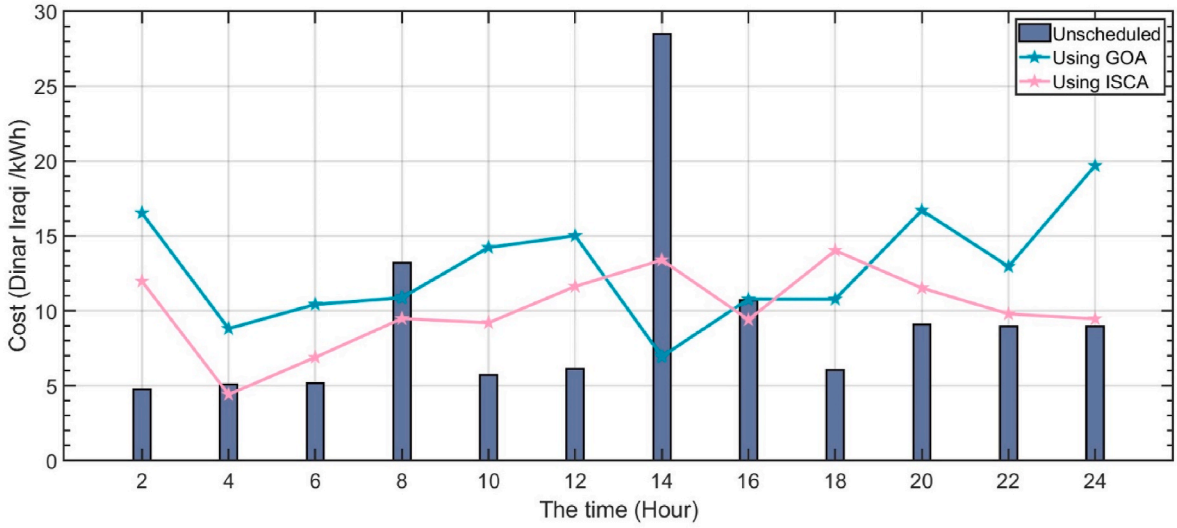

Fig. 15. The cost of electricity for RTP.

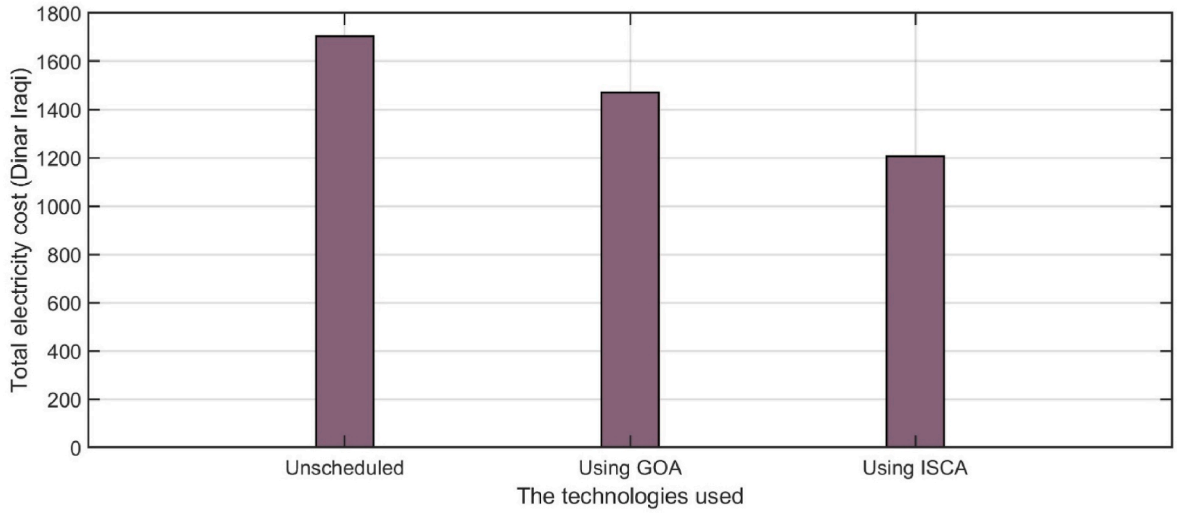

Fig. 16. Total electricity cost using different technologies.

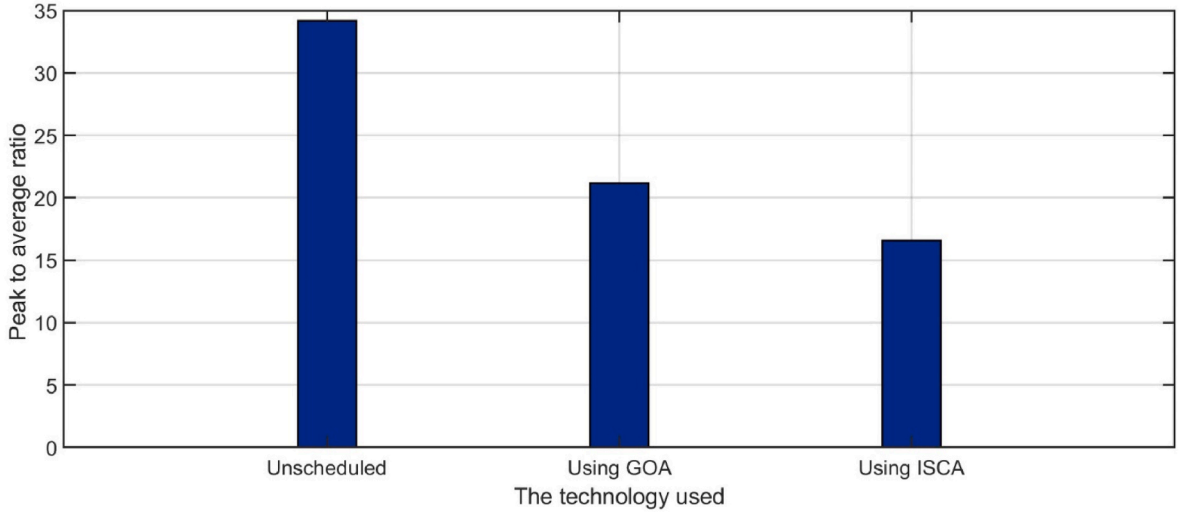

Fig. 17. PAR using different technologies.

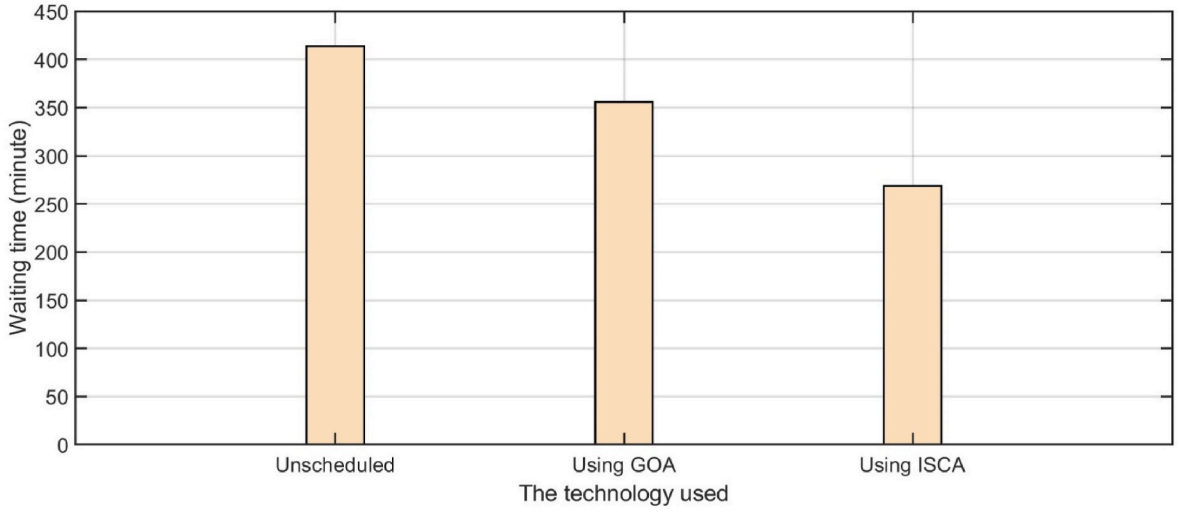

Fig. 18. Waiting time using different technologies.

devices (e.g electric vehicles) to reconstruct the distributed energy generation from the perspective of energy conservation and carbon reduction, and combining big data and artificial intelligence automatic analysis through intelligent technology to form a model of "Smart Urban Buildings photovoltaic + Smart Urban Buildings energy storage + electric vehicles".

CRediT authorship contribution statement

Bilal Naji Alhasnawi: Software, Resources, Methodology, Investigation, Formal analysis, Data curation, Conceptualization. **Basil H. Jasim:** Writing – review & editing. **Arshad Naji Alhasnawi:** Writing – review & editing. **Firas Faeq K. Hussain:** Writing – review & editing. **Raad Z. Homod:** Writing – review & editing. **Husam Abdulrasool Hasan:** Writing – review & editing. **Osamah Ibrahim Khalaf:** Writing – review & editing. **Rabeh Abbassi:** Writing – review & editing. **Bahamin Bazooyar:** Software, Resources, Methodology, Investigation, Formal analysis, Data curation, Conceptualization. **Marek Zanker:** Writing – review & editing, Visualization, Supervision, Software, Resources, Project administration. **Vladimír Bureš:** Writing – review & editing, Visualization, Supervision, Software, Resources, Project administration. **Bishoy E. Sedhom:** Writing – review & editing.

Declaration of competing interest

The authors declare that they have no known competing financial interests or personal relationships that could have appeared to influence the work reported in this paper.

Data availability

The data used for this research and prepatation of this article can be accessed from Brunel University of London repository at: https://doi.org/10.17633/rd.brunel.26049436.v1.

Acknowledgments

The research has been partially supported by the Faculty of Informatics and Management UHK excellence project "Methodological perspectives on modeling and simulation of hard and soft systems".

References

[1] A.C. Duman, H.S. Erden, Ö. Gönül, Ö. Güler, A home energy management system with an integrated smart thermostat for demand response in smart grids, Sustain. Cities Soc. 65 (2021) 102639, https://doi.org/10.1016/j.scs.2020.102639.

[2] S. Dixit, P. Singh, J. Ogale, P. Bansal, Y. Sawle, Energy management in microgrids with renewable energy sources and demand response, Comput. Electr. Eng. 110 (2023) 108848, https://doi.org/10.1016/j.compeleceng.2023.108848.

[3] G.R. Aghajani, H.A. Shayanfar, H. Shayeghi, Presenting a multi-objective generation scheduling model for pricing demand response rate in MG energy management, Energy Convers. Manag. 106 (2015) 308–321, https://doi.org/10.1016/j.enconman.2015.08.059.

[4] B. Dey, F. Pedro García Márquez, A. Bhattacharya, Demand side management as a mandatory inclusion for economic operation of rural and residential microgrid systems, Sustain. Energy Technol. Assessments 54 (2022) 102903, https://doi.org/10.1016/j.seta.2022.102903.

[5] N.R. Babu, T. Chiranjeevi, L.C. Saikia, D.K. Raju, Optimization solutions for demand side management, in: H. Malik, A. Iqbal, P. Joshi, S. Agrawal, F.I. Bakhsh (Eds.), Metaheuristic and Evolutionary Computation: Algorithms and Applications, Studies in Computational Intelligence, vol 916, Springer, Singapore, 2021, https://doi.org/10.1007/978-981.

[6] Md Juel Rana, Forhad Zaman, Tapabrata Ray, Ruhul Sarker, Real-time scheduling of community microgrid, J. Clean. Prod. 286 (2021) 125419.

[7] A. Khajehzadeh, M. Jahromi, M. Mahmoudian, E. Rodrigues, R. Melicio, Novel control framework for optimal scheduling in microgrid with demand response support under contingency events, Cleaner Energy Systems 3 (2022) 100019, https://doi.org/10.1016/j.cles.2022.100019.

[8] Fahad R. Albogamy, Yasir Ashfaq, Ghulam Hafeez, Sadia Murawwat, Sheraz Khan, Faheem Ali, Farrukh Aslam Khan, Khalid Rehman, Optimal demand-side management using flat pricing scheme in smart grid, Processes 10 (6) (2022) 1214, https://doi.org/10.3390/pr10061214.

[9] Faran Asghar, Adnan Zahid, Muhammad Imtiaz Hussain, Furqan Asghar, Waseem Amjad, Jun-Tae Kim, A novel solution for optimized energy management systems comprising an AC/DC hybrid microgrid system for industries, Sustainability 14 (14) (2022) 8788, https://doi.org/10.3390/su14148788.

[10] Bilal Naji Alhasnawi, Basil H. Jasim, Arshad Naji Alhasnawi, Bishoy E. Sedhom, Ali M. Jasim, Azam Khalili, Vladimír Bureš, Alessandro Burgio, Pierluigi Siano, A novel approach to achieve MPPT for photovoltaic system based SCADA, Energies 15 (22) (2022) 8480, https://doi.org/10.3390/en15228480.

[11] M Jasim Ali, Basil H. Jasim, Bogdan-Constantin Neagu, Bilal Naji Alhasnawi, Efficient optimization algorithm-based demand-side management program for smart grid residential load, Axioms 12 (1) (2023) 33, https://doi.org/10.3390/axioms12010033.

[12] B.N. Alhasnawi, B.H. Jasim, A. Anvari-Moghaddam, F. Blaabjerg, A new robust control strategy for parallel operated inverters in green energy applications, Energies 13 (2020) 3480, https://doi.org/10.3390/en13133480.

[13] M Jasim Ali, Basil H. Jasim, Bogdan-Constantin Neagu, Bilal Naji Alhasnawi, Coordination control of a hybrid AC/DC smart microgrid with online fault detection, diagnostics, and localization using artificial neural networks, Electronics 12 (1) (2023) 187, https://doi.org/10.3390/electronics12010187.

[14] Bilal Naji Alhasnawi, Basil H. Jasim, Bishoy E. Sedhom, Distributed secondary consensus fault tolerant control method for voltage and frequency restoration and power sharing control in multi-agent microgrid, Int. J. Electr. Power Energy Syst. 133 (December 2021) 107251.

[15] Bilal Naji Alhasnawi, Basil H. Jasim, Walid Issa, M. Dolores Esteban, A novel cooperative controller for inverters of smart hybrid AC/DC microgrids, Appl. Sci. 10 (17) (2020) 6120, https://doi.org/10.3390/app10176120.

[16] Q. Li, Z. Cui, Y. Cai, Y. Su, B. Wang, Renewable-based microgrids' energy management using smart deep learning techniques: realistic digital twin case, Sol. Energy 250 (2023) 128–138, https://doi.org/10.1016/j.solener.2022.12.030.

[17] M. Tostado-Véliz, P. Arévalo, S. Kamel, H.M. Zawbaa, F. Jurado, Home energy management system considering effective demand response strategies and uncertainties, Energy Rep. 8 (2022) 5256–5271, https://doi.org/10.1016/j.egyr.2022.04.006.

[18] B. Alhasnawi, B. Jasim, Z.-A. Rahman, J. Guerrero, M. Esteban, A novel internet of energy based optimal multi-agent control scheme for microgrid including renewable energy resources, Int. J. Environ. Res. Publ. Health 18 (2021) 8146, https://doi.org/10.3390/ijerph18158146.

[19] Bilal Naji Alhasnawi, Basil H. Jasim, Internet of Things (IoT) for smart grids: a comprehensive review, J. Xi'an Univ. Archit 63 (2020) 1006–7930.

[20] Zain-Aldeen SA. Rahman, Basil H. Jasim, Yasir IA. Al-Yasir, Yim-Fun Hu, Raed A. Abd-Alhameed, Bilal Naji Alhasnawi, A new fractional-order chaotic system with its analysis, synchronization, and circuit realization for secure communication applications, Mathematics 9 (20) (2021) 2593, https://doi.org/10.3390/math9202593.

[21] Wenjing Zhang, Hong Qiao, Xianyong Xu, Junxingxu Chen, Jian Xiao, Keren Zhang, Yanbo Long, YuanJun Zuo, Energy management in microgrid based on deep reinforcement learning with expert knowledge. Proc. SPIE 12492, International Workshop on Automation, Control, and Communication Engineering (IWACCE 2022), 9 December 2022 124920Z, https://doi.org/10.1117/12.2662727.

[22] B.N. Alhasnawi, B.H. Jasim, R. Mansoor, A.N. Alhasnawi, Z.-A.S.A. Rahman, H. Haes Alhelou, J.M. Guerrero, A.M. Dakhil, P. Siano, A new Internet of Things based optimization scheme of residential demand side management system, IET Renew. Power Gener. (2022) 1–15, https://doi.org/10.1049/rpg2.12466.

[23] Zain-Aldeen SA. Rahman, Basil H. Jasim, Yasir IA. Al-Yasir, Raed A. Abd-Alhameed, Bilal Naji Alhasnawi, A new no equilibrium fractional order chaotic system, dynamical investigation, synchronization, and its digital implementation, Inventions 6 (3) (2021) 49, https://doi.org/10.3390/inventions6030049.

[24] B.N. Alhasnawi, B.H. Jasim, B.E. Sedhom, E. Hossain, J.M. Guerrero, A new decentralized control strategy of microgrids in the internet of energy paradigm, Energies 14 (2021) 2183, https://doi.org/10.3390/en14082183.

[25] J.S. Vardakas, N. Zorba, C.V. Verikoukis, Power demand control scenarios for smart grid applications with finite number of appliances, Appl. Energy 162 (2016) 83–98, https://doi.org/10.1016/j.apenergy.2015.10.008.

[26] C. Li, X. Yu, W. Yu, G. Chen, J. Wang, Efficient computation for sparse load shifting in demand side management, IEEE Trans. Smart Grid 8 (2017) 250–261.

[27] Bilal Naji Alhasnawi, Basil H. Jasim, Pierluigi Siano, Hassan Haes Alhelou, Amer Al-Hinai, A novel solution for day-ahead scheduling problems using the IoT-based bald eagle search optimization algorithm, Inventions 7 (3) (2022) 48, https://doi.org/10.3390/inventions7030048.

[28] Jitendra Vagdoda, Darshan Makwana, Amit Adhikaree, Tasnimun Faika, Taesic Kim, A Cloud-Based Multiagent System Platform for Residential Microgrids towards Smart Grid Community, IEEE Power & Energy Society General Meeting (PESGM), Portland, OR, USA, 24 December 2018.

[29] D. Bahmanyar, N. Razmjooy, S. Mirjalili, Multi-objective scheduling of IoT-enabled smart homes for energy management based on Arithmetic Optimization Algorithm: a Node-RED and NodeMCU module-based technique, Knowl. Base Syst. 247 (2022) 108762, https://doi.org/10.1016/j.knosys.2022.108762.

[30] Y. Wang, T. -L. Nguyen, Y. Xu, Q. -T. Tran, R. Caire, Peer-to-Peer Control for Networked Microgrids: Multi-Layer and Multi-Agent Architecture Design," in, IEEE Transactions on Smart Grid 11 (6) (Nov. 2020) 4688–4699, https://doi.org/10.1109/TSG.2020.3006883.

[31] K. Wang, H. Li, S. Maharjan, Y. Zhang, S. Guo, Green energy scheduling for demand side Management in the Smart Grid, IEEE Transactions on Green Communications and Networking 2 (2) (June 2018).

[32] B.N. Alhasnawi, B.H. Jasim, SCADA controlled smart home using Raspberry Pi3, in: Proceedings of the 2018 International Conference on Advance of Sustainable Engineering and its Application (ICASEA), Wasit-Kut, Iraq, 2018, https://doi.org/10.1109/ICASEA.2018.8370946.

[33] M.H.Y. Moghaddam, A. Leon-Garcia, A fog-based internet of energy architecture for Transactive energy management systems, IEEE Internet Things J. 5 (2) (2018) 1055–1069.

[34] B.N. Alhasnawi, B.H. Jasim, A new energy management system of on-grid/off-grid using adaptive neuro-fuzzy inference system, J. Eng. Sci. Technol. 15 (2020) 3903–3919.

[35] S.A. Hashmi, C.F. Ali, S. Zafar, Internet of things and cloud computing based energy management system for demand-side management in smart grid, Int. J. Energy Res. (2020) 1–16.

[36] Sima Davarzani, Ramon Granella, Gareth A. Taylor, Ioana Pisica, Implementation of a novel multi-agent system for demand response management in low-voltage distribution networks, Appl. Energy 253 (1) (2019) 113–516.

[37] B.N. Alhasnawi, B.H. Jasim, A novel hierarchical energy management system based on optimization for multi-microgrid, Int. J. Electr. Eng. Inform. 12 (2020) 586–606.

[38] Hessam Golmohamadi, Reza Keypour, Birgitte Bak-Jensen, Jayakrishnan R. Pillai, A multi-agent based optimization of residential and industrial demand response aggregators, Int. J. Electr. Power Energy Syst. 107 (2019) 472–485.

[39] Cortes-Arcos, "T. Multi-objective demand response to real-time prices (RTP) using a task scheduling methodology", Energy 138 (2017) 19–31.

[40] B.N. Alhasnawi, B.H. Jasim, M.D. Esteban, J.M. Guerrero, A novel smart energy management as a service over a cloud computing platform for nanogrid appliances, Sustain. J. Rec. 12 (2020) 9686, https://doi.org/10.3390/su12229686.

[41] B.N. Alhasnawi, B.H. Jasim, Adaptive energy management system for smart hybrid microgrids, in: Proceedings of the 3rd Scientific Conference of Electrical and Electronic Engineering Research (SCEEER), Basrah, Iraq, June 2020, pp. 15–16, https://doi.org/10.37917/ijeee.sceeer.3rd.11.

[42] A.R. Al-Ali, Imran A. Zualkernan, Mohammed Rashid, Ragini Gupta, Mazin AliKarar, A smart home energy management system using IoT and big data analytics approach, IEEE Trans. Consum. Electron. 63 (4) (2017) 426–434.

[43] Z. Huang, F. Wang, Y. Lu, X. Chen, Q. Wu, Optimization model for home energy management system of rural dwellings, Energy 283 (2023) 129039, https://doi.org/10.1016/j.energy.2023.129039.

[44] M.S. Ahmed, A. Mohamed, T. Khatib, H. Shareef, R.Z. Homod, J.A. Ali, Real time optimal schedule controller for home energy management system using new binary backtracking search algorithm, Elsevier Energy and Build 138 (2017) 215–227.

[45] Masoud Ahmadipour, Muhammad Murtadha Othman, Zainal Salam, Moath Alrifaey, Hussein Mohammed Ridha, Veerapandiyan Veerasamy, Optimal load shedding scheme using grasshopper optimization algorithm for islanded power system with distributed energy resources, Ain Shams Eng. J. (28 May 2022) 101835.

[46] Chinmaya Mahapatra, Akshaya Kumar Moharana, Victor M. Leung, Energy management in smart cities based on internet of things: peak demand reduction and energy savings, Sensors 17 (12) (2017) 2812.

[47] B. Alhasnawi, B. Jasim, P. Siano, J. Guerrero, A novel real-time electricity scheduling for home energy management system using the internet of energy, Energies 14 (2021) 3191, https://doi.org/10.3390/en14113191.

[48] Mohammad Abdullah Al Faruque, Korosh Vatanparvar, Energy management-as-a-service over fog computing platform, IEEE Internet Things J. 3 (2) (2016) 161–169.

[49] W.X. Li, T. Logenthiran, V.T. Phan, W.L. Woo, Implemented IoT based self-learning home management system (SHMS) for Singapore, IEEE Internet Things J. 5 (3) (2018) 2212–2219.

[50] B.N. Alhasnawi, B.H. Jasim, M.D. Esteban, A new robust energy management and control strategy for a hybrid microgrid system based on green energy, Sustain. J. Rec. 12 (2020) 5724, https://doi.org/10.3390/su12145724.

[51] Zia Ullah, Shoarong Wang, Guoan Wu, Mengmeng Xiao, Jinmu Lai, Mohamed R. Elkadeem, Advanced energy management strategy for microgrid using real-time monitoring interface, J. Energy Storage 52 (Part A) (2022) 104814.

[52] Khac-Hoai Nam Bui, Jason J. Jung, David Camacho, Consensual negotiation-based decision making for connected appliances in smart home management systems, Sensors 18 (7) (2018) 2206, https://doi.org/10.3390/s18072206.

[53] Ateeq Ur Rehman, Ghulam Hafeez, Fahad R. Albogamy, Zahid Wadud, Faheem Ali, Imran Khan, Gul Rukh, And Sheraz Khan, "An efficient energy management in smart grid considering demand response program and renewable energy sources", IEEE Access (Volume: 9), Page(s): 148821 - 148844, DOI: 10.1109/ACCESS.2021.3124557.

[54] B.N. Alhasnawi, B.H. Jasim, A.M. Jasim, V. Bureš, A.N. Alhasnawi, R.Z. Homod, M. R.M. Alsemawai, R. Abbassi, B.E. Sedhom, A multi-objective improved cockroach swarm algorithm approach for apartment energy management systems, Information 14 (2023) 521, https://doi.org/10.3390/info14100521.

[55] Amir Ali Dashtaki, Morteza Khaki, Mohammad Zand, Mostafa Azimi Nasab, P. Sanjeevikumar, Tina Samavat, Morteza Azimi Nasab, and Baseem Khan, " A Day Ahead Electrical Appliance Planning of Residential Units in a Smart Home Network Using ITS-BF Algorithm", Hindawi, International Transactions on Electrical Energy Systems Volume 2022, Article ID 2549887, 13 pages https://doi.org/10.1155/2022/2549887.

[56] Bilal Naji Alhasnawi, Basil H. Jasim, Zain-Aldeen S.A. Rahman, Pierluigi Siano, A novel robust smart energy management and demand reduction for smart homes based on internet of energy, Sensors 21 (14) (2021) 4756, https://doi.org/10.3390/s21144756.

[57] R. Abbassi, M. Hammami, S. Chebbi, Improvement of the integration of a grid-connected wind-photovoltaic hybrid system, in: Proceedings of the International Conference on Electrical Engineering and Software Applications, Yasmine Hammamet, Tunisia, March 2013, pp. 17–19.

[58] Z. Lijun, J. Houssem, A. Rabeh, L. Bin, L. Mohsen, N. Hiroki, Sizing renewable energy systems with energy storage systems based microgrids for cost minimization using hybrid shuffled frog-leaping and pattern search algorithm, Sustain. Cities Soc. 73 (2021) 103124.

[59] L. Ning, S. Zhanguo, J. Houssem, A. Rabeh, L. Mohsen, F. Noritoshi, Energy management and optimized operation of renewable sources and electric vehicles based on microgrid using hybrid gravitational search and pattern search algorithm, Sustain. Cities Soc. 75 (2021) 103279.

[60] T. Suqiong, J. Mingxin, A. Rabeh, J. Houssem, L. Mohsen, A cost-oriented resource scheduling of a solar-powered microgrid by using the hybrid crow and pattern search algorithm, J. Clean. Prod. 313 (2021) 127853.

[61] R. Abbassi, S. Saidi, A. Abbassi, H. Jerbi, M. Kchaou, B.N. Alhasnawi, Accurate key parameters estimation of PEMFCs' models based on dandelion optimization algorithm, Mathematics 11 (2023) 1298.

[62] Abbassi, A.; Mehrez, RB.; Abbassi, R.; Saidi, S.; Albdran, S.; Jemli, M. Improved off-grid wind/photovoltaic/hybrid energy storage system based on new framework of Moth-Flame optimization algorithm. Int. J. Energy Res. 46 (5), 6711-6729..

[63] A. Albaker, M. Alturki, R. Abbassi, K. Alqunun, Zonal-based optimal microgrids identification, Energies 15 (2022) 2446.

[64] A. Bassam, A. Rabeh, A. Hani, A. Badr, J. Houssem, A. Saleh, Flexible control of grid-connected renewable energy systems inverters under unbalanced grid faults, International Journal of Advanced and Applied Sciences 9 (9) (2022) 53–60.

[65] N. Yin, R. Abbassi, H. Jerbi, A. Rezvani, M. Müller, A day-ahead joint energy management and battery sizing framework based on θ-modified krill herd algorithm for a renewable energy-integrated microgrid, J. Clean. Prod. 282 (2021) 124435.

[66] M. Alturki, R. Abbassi, A. Albaker, H. Jerbi, A new hybrid synchronization PLL scheme for interconnecting renewable energy sources to an abnormal electric grid, Mathematics 10 (2022) 1101.

[67] A. Abdelkader, R. Abbassi, H. Ali, O. Diego, C. Huiling, H. Arslan, J. Mohamed, W. Mingjing, Parameters identification of photovoltaic cell models using enhanced exploratory salp chains-based approach, Energy 198 (2020) 117333.

[68] G. Shaolei, A. Rabeh, J. Houssem, R. Alireza, S. Kengo, Efficient maximum power point tracking for a photovoltaic using hybrid shuffled frog-leaping and pattern search algorithm under changing environmental conditions, J. Clean. Prod. 297 (2021) 126573.

[69] A. Rabeh, A. Abdelkader, J. Mohamed, C. Souad, Identification of unknown parameters of solar cell models: a comprehensive overview of available approaches, Renew. Sustain. Energy Rev. 90 (2018) 453–474.

[70] A. Rabeh, A. Boudjemline, A. Abdelkader, A. Torchani, H. Gasmi, T. Guesmi, A numerical-analytical hybrid approach for the identification of SDM solar cell unknown parameters, Eng. Technol. Appl. Sci. Res. 8 (3) (2018) 2907–2913.

[71] R. Abbassi, S. Saidi, A. Abbassi, H. Jerbi, M. Kchaou, B.N. Alhasnawi, Accurate key parameters estimation of PEMFCs' models based on dandelion optimization algorithm, Mathematics 11 (2023) 1298.

[72] Oussama Ouramdane, Elhoussin Elbouchikhi, Yassine Amirat, Franck Le Gall, Ehsan Sedgh Gooya, Home energy management considering renewable resources, energy storage, and an electric vehicle as a backup, Energies 15 (8) (2022) 2830, https://doi.org/10.3390/en15082830.

[73] B.N. Alhasnawi, B.H. Jasim, B.E. Sedhom, J.M. Guerrero, Consensus algorithm-based coalition game theory for demand management scheme in smart microgrid, Sustain. Cities Soc. 74 (2021) 103248, https://doi.org/10.1016/j.scs.2021.103248.

[74] Bilal Naji Alhasnawi, Basil H. Jasim, " A new coordinated control of hybrid microgrids with renewable energy resources under variable loads and generation conditions", Iraqi Journal for Electrical & Electronic Engineering 16 (2) (2020).

[75] Adriana C. Luna, Nelson L. Diaz, Moisès Graells, Juan C. Vasquez, Josep M. Guerrero, "Mixed-Integer-Linear-Programming-Based energy management system for hybrid PV-Wind-Battery microgrids: modeling, design, and experimental verification ", IEEE Trans. Power Electron. 32 (4) (April 2017) https://doi.org/10.1109/TPEL.2016.2581021.

[76] B.N. Alhasnawi, B.H. Jasim, V. Bureš, B.E. Sedhom, A.N. Alhasnawi, R. Abbassi, M. R.M. Alsemawai, P. Siano, J.M. Guerrero, A novel economic dispatch in the stand-alone system using improved butterfly optimization algorithm, Energy Strategy Rev. 49 (2023) 101135, https://doi.org/10.1016/j.esr.2023.101135.

[77] Zafar Iqbal, On Optimizing Energy Consumption with Combined Operations of Microgrids for Demand Side Management in Smart Homes, Arid Agriculture University Rawalpindi, Pakistan, 2018. Ph.D. Thesis, University Institute Of Information Technology, Pir Mehr Ali Shah.

[78] Omar Alrumayh; Kankar Bhattacharya, "Flexibility of residential loads for demand response provisions in smart grid ", IEEE Trans. Smart Grid (Volume: 10, Issue: 6, November 2019), Page(s): 6284 - 6297, DOI: 10.1109/TSG.2019.2901191.

[79] Yaling Chen, Luxi Hao, and Gaowen Yin, "Distributed Energy Management of the Hybrid AC/DC Microgrid with High Penetration of Distributed Energy Resources Based on ADMM", Hindawi, Complexity, Volume 2021, Article ID 1863855, 9 pages, https://doi.org/10.1155/2021/1863855.

[80] Z. Song, X. Guan, M. Cheng, Multi-objective optimization strategy for home energy management system including PV and battery energy storage, Energy Rep. 8 (2022) 5396–5411, https://doi.org/10.1016/j.egyr.2022.04.023.

[81] A. Rahman, T. Aziz, N. Masood, S.R. Deeba, A time of use tariff scheme for demand side management of residential energy consumers in Bangladesh, Energy Rep. 7 (2021) 3189–3198, https://doi.org/10.1016/j.egyr.2021.05.042.

[82] M.I. El-Afifi, B.E. Sedhom, A.A. Eladl, M. Elgamal, P. Siano, Demand side management strategy for smart building using multi-objective hybrid optimization technique, Results in Engineering 22 (2024) 102265, https://doi.org/10.1016/j.rineng.2024.102265.

[83] A. Atefi, V. Gholaminia, Flexible demand-side management program in accordance with the consumers' requested constraints, Energy Build. 309 (2024) 114013, https://doi.org/10.1016/j.enbuild.2024.114013.

[84] S. Balavignesh, C. Kumar, S. Ueda, T. Senjyu, Optimization-based optimal energy management system for smart home in smart grid, Energy Rep. 10 (2023) 3733–3756, https://doi.org/10.1016/j.egyr.2023.10.037.

[85] Y. Liu, Y. Bao, Intelligent monitoring of spatially-distributed cracks using distributed fiber optic sensors assisted by deep learning, Measurement 220 (2023) 113418, https://doi.org/10.1016/j.measurement.2023.113418.

[86] Y. Liu, Y. Bao, Review on automated condition assessment of pipelines with machine learning, Adv. Eng. Inf. 53 (2022) 101687, https://doi.org/10.1016/j.aei.2022.101687.

[87] Ziqian Luo, Hua Xu, Feiyang Chen, Audio Sentiment Analysis by Heterogeneous Signal Features Learned from Utterance-Based Parallel Neural Network, 2018. AffCon@AAAI.

[88] Feiyang Chen, Ziqian Luo, Yanyan Xu, Complementary Fusion of Multi-Features and Multi-Modalities in Sentiment Analysis, 2019. AffCon@AAAI.

[89] Z. Luo, X. Zeng, Z. Bao, M. Xu, Deep learning-based strategy for macromolecules classification with imbalanced data from cellular electron cryotomography, in: 2019 International Joint Conference on Neural Networks (IJCNN), 2019, pp. 1–8, https://doi.org/10.1109/IJCNN.2019.8851972. Budapest, Hungary.

[90] L. Yi, G. Li, K. Chen, Q. Liu, J. Liu, Optimal scheduling of residential houses with optimal photovoltaic energy utilization strategy using improved multi-objective equilibrium optimizer algorithm, J. Build. Eng. 59 (2022) 105102, https://doi.org/10.1016/j.jobe.2022.105102.

[91] B.N. Alhasnawi, B.H. Jasim, A new internet of things enabled trust distributed demand side management system, Sustain. Energy Technol. Assessments 46 (2021) 101272.

[92] B.E. Sedhom, M.M. El-Saadawi, M. El Moursi, M. Hassan, A.A. Eladl, IoT-based optimal demand side management and control scheme for smart microgrid, Int. J. Electr. Power Energy Syst. 127 (2021) 106674, https://doi.org/10.1016/j.ijepes.2020.106674.

[93] F.R. Albogamy, S.A. Khan, G. Hafeez, S. Murawwat, S. Khan, S.I. Haider, A. Basit, K.-D. Thoben, Real-time energy management and load scheduling with renewable energy integration in smart grid, Sustainability 14 (2022) 1792, https://doi.org/10.3390/su14031792.

[94] Adia Khalid, Towards Energy Efficiency in Smart Buildings Exploiting Dynamic Coordination Among Appliances and Homes, Computer Science COMSATS University, Islamabad, Islamabad, Pakistan, Spring, 2018. PhD Thesis.

[95] M. Ahmadipour, M. Murtadha Othman, Z. Salam, M. Alrifaey, H. Mohammed Ridha, V. Veerasamy, Optimal load shedding scheme using grasshopper optimization algorithm for islanded power system with distributed energy resources, Ain Shams Eng. J. 14 (1) (2023) 101835, https://doi.org/10.1016/j.asej.2022.101835.

[96] S. Mirjalili, SCA: a Sine Cosine Algorithm for solving optimization problems, Knowl. Base Syst. 96 (2016) 120–133, https://doi.org/10.1016/j.knosys.2015.12.022.

[97] S. Gupta, K. Deep, Improved sine cosine algorithm with crossover scheme for global optimization, Knowl. Base Syst. 165 (2019) 374–406, https://doi.org/10.1016/j.knosys.2018.12.008.

[98] S. Mohseni, A.C. Brent, Probabilistic sizing and scheduling co-optimisation of hybrid battery/super-capacitor energy storage systems in micro-grids, J. Energy Storage 73 (2023) 109172, https://doi.org/10.1016/j.est.2023.109172.

[99] S. Mirjalili, Moth-flame optimization algorithm: a novel nature-inspired heuristic paradigm, Knowl. Base Syst. 89 (2015) 228–249, https://doi.org/10.1016/j.knosys.2015.07.006.